3

$O(n)$ models

In this chapter we study scalar field models with $O(n)$ symmetry described by the Euclidean action

$$S = -\int d^4x \left[\tfrac{1}{2}\partial_\mu\varphi^\alpha\partial_\mu\varphi^\alpha + \tfrac{1}{2}\mu^2\varphi^\alpha\varphi^\alpha + \tfrac{1}{4}\lambda(\varphi^\alpha\varphi^\alpha)^2\right], \tag{3.1}$$

where $\varphi^\alpha(x) = \alpha = 0, \ldots, n-1$ is an n-vector in 'internal space'. The action is invariant under $O(n)$, the group of orthogonal transformations in n dimensions. For $n = 4$ this action describes the scalar Higgs sector of the Standard Model. It can also be used as an effective low-energy action for pions. Since the models are relatively simple they serve as a good arena for illustrating scaling and universality, concepts of fundamental importance in quantum field theory.

It turns out that scalar field models (in four dimensions) become 'trivial' in the sense that the interactions disappear very slowly when the lattice distance is taken to zero. The interpretation and implication of this interesting phenomenon will be also be discussed.

3.1 Goldstone bosons

We have seen in section 1.2 that the one-component classical scalar field (i.e. $n = 1$) can be in two different phases, depending on the sign of μ^2, namely a 'broken phase' in which the ground-state value $\varphi_{\rm g} \neq 0$, and a 'symmetric phase' in which $\varphi_{\rm g} = 0$. For $n > 1$ there are also two phases and we shall see that in the case of continuous internal symmetry the consequence of spontaneous symmetry breaking is the appearance of massless particles, called Goldstone bosons.†

† Actually, this is true in space–time dimensions ≥ 3. In one and two space–time dimensions spontaneous breaking of a continuous symmetry is not possible (Merwin–Wagner theorem, Coleman's theorem).

https://doi.org/10.1017/9781009402705.004 Published online by Cambridge University Press

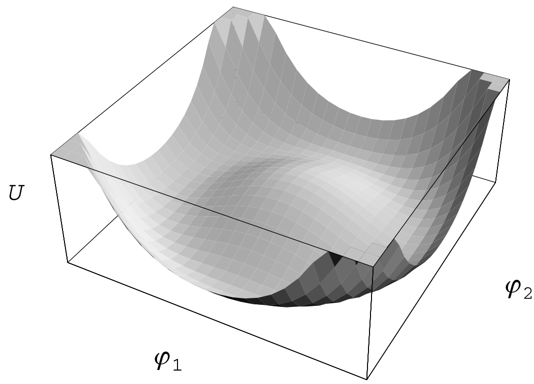

Fig. 3.1. Shape of U for $n = 2$ for $\mu^2 < 0$.

The potential

$$U = \frac{1}{2}\mu^2\varphi^2 + \frac{1}{4}\lambda(\varphi^2)^2 \tag{3.2}$$

has a 'wine-bottle-bottom' shape, also called 'Mexican-hat' shape, if $\mu^2 < 0$ (figure 3.1). It is clear that for $\mu^2 > 0$ the ground state is unique ($\varphi_{\mathrm{g}} = 0$) but that for $\mu^2 < 0$ it is infinitely degenerate. The equation $\partial U/\partial\varphi^k = 0$ for the minima, $(\mu^2 + \lambda\varphi^2)\varphi^\alpha = 0$, has the solution

$$\varphi_{\mathrm{g}}^\alpha = v\delta_{\alpha,0}, \quad v^2 = -\mu^2/\lambda \quad (\mu^2 < 0), \tag{3.3}$$

or any $O(n)$ rotation of this vector. To force the system into a definite ground state we add a symmetry-breaking term to the action (the same could be done in the one-component φ^4 model),

$$\Delta S = \int dx\, \epsilon\varphi^0(x), \quad \epsilon > 0. \tag{3.4}$$

The constant ϵ has the dimension of (mass)^3. The equation for the stationary points now reads

$$(\mu^2 + \lambda\varphi^2)\varphi^\alpha = \epsilon\delta_{\alpha 0}. \tag{3.5}$$

With the symmetry breaking (3.4) the ground state has $\varphi_{\mathrm{g}}^\alpha$ pointing in the $\alpha = 0$ direction,

$$\varphi_{\mathrm{g}}^\alpha = v\delta_{\alpha 0}, \quad (\mu^2 + \lambda v^2)v = \epsilon. \tag{3.6}$$

Consider now small fluctuations about φ_{g}. The equations of motion (field equations) read

$$(-\partial^2 + \mu^2 + \lambda\varphi^2)\varphi^\alpha = \epsilon\delta_{\alpha 0}, \quad \partial^2 \equiv \nabla^2 - \partial_t^2. \tag{3.7}$$

https://doi.org/10.1017/9781009402705.004 Published online by Cambridge University Press

Linearizing around $\varphi = \varphi_{\rm g}$, writing

$$\varphi^0 = v + \sigma, \quad \varphi^k = \pi_k, \quad k = 1, \ldots, n-1, \tag{3.8}$$

we find

$$(-\partial^2 + m_\sigma^2)\sigma = 0, \quad (-\partial^2 + m_\pi^2)\pi_k = 0, \tag{3.9}$$

with

$$m_\sigma^2 = \mu^2 + 3\lambda v^2 = 2\lambda v^2 + \epsilon/v, \tag{3.10}$$
$$m_\pi^2 = \mu^2 + \lambda v^2 = \epsilon/v. \tag{3.11}$$

For $\mu^2 > 0$, $v = 0$ and $m_\sigma^2 = m_\pi^2 = \mu^2$, whereas for $\mu^2 < 0$, $v > 0$ and the σ particle is heavier than the π particles. For $\epsilon \to 0$ the π particles become *massless*,

$$m_\pi^2 \approx \epsilon/v_0 \to 0, \quad v_0 = v_{|\epsilon=0}. \tag{3.12}$$

The simple effective $O(n)$ model reproduces the important features of Goldstone's theorem: spontaneous symmetry breaking of a continuous symmetry leads to massless particles, the Goldstone bosons. For small explicit symmetry breaking the Goldstone bosons get a squared mass proportional to the strength of the breaking. The massless modes correspond to oscillations along the vacuum valley of the 'Mexican hat'.

As mentioned earlier, the $O(4)$ model is a reasonable model for the effective low-energy interactions of pions amongst themselves. The particles $\pi^\pm$ and π^0 are described by the fields $\pi_k(x)$. The σ field (after which the model is named the σ model) corresponds to the very broad σ resonance around 900 MeV. The model loses its validity at such energies, for example the ρ mesons with mass 770 MeV are completely neglected.

3.2 $O(n)$ models as spin models

We continue in the quantum theory. The lattice regularized action will be taken as

$$S = -\sum_x \left[\tfrac{1}{2}\partial_\mu\varphi_x^\alpha\partial_\mu\varphi_x^\alpha + \tfrac{1}{2}m_0^2\varphi_x^\alpha\varphi_x^\alpha + \tfrac{1}{4}\lambda_0(\varphi_x^\alpha\varphi_x^\alpha)^2\right]. \tag{3.13}$$

We have changed the notation for the parameters: $\mu^2 \to m_0^2$, $\lambda \to \lambda_0$. The subscript 0 indicates that these are 'bare' or 'unrenormalized' parameters that differ from the physical 'dressed' or 'renormalized' values which are measured in experiments.

We shall mostly use lattice units, $a = 1$. Using $\partial_\mu \varphi_x^\alpha = \varphi_{x+\hat{\mu}}^\alpha - \varphi_x^\alpha$, the action can be rewritten in the form

$$S = \sum_{x\mu} \varphi_x^\alpha \varphi_{x+\hat{\mu}}^\alpha - \sum_x \left[\tfrac{1}{2}(2d + m_0^2)\varphi^2 + \tfrac{1}{4}\lambda_0(\varphi^2)^2\right], \tag{3.14}$$

where d is the number of space–time dimensions. Another standard choice of parameters is obtained by writing

$$\varphi^\alpha = \sqrt{2\kappa}\,\phi^\alpha, \quad m_0^2 = \frac{1-2\lambda}{\kappa} - 2d, \quad \lambda_0 = \frac{\lambda}{\kappa^2}, \tag{3.15}$$

which brings S into the form

$$S = 2\kappa \sum_{x\mu} \phi_x^\alpha \phi_{x+\hat{\mu}}^\alpha - \sum_x \left[\,\phi_x^\alpha \phi_x^\alpha + \lambda(\phi_x^\alpha \phi_x^\alpha - 1)^2\right]. \tag{3.16}$$

The partition function is given by

$$Z = \left(\prod_{x\alpha} \int_{-\infty}^{\infty} d\phi_x^\alpha\right) \exp S \equiv \int D\mu(\phi) \exp\left(2\kappa \sum_{x\mu} \phi_x \phi_{x+\hat{\mu}}\right), \tag{3.17}$$

where we have introduced an integration measure $D\mu(\phi)$, which is the product of probability measures $d\mu(\phi)$ for a single site,

$$D\mu(\phi) = \prod_x d\mu(\phi_x), \quad d\mu(\phi) = d^n\phi\, \exp[\,-\phi^2 - \lambda(\phi^2 - 1)^2\,]. \tag{3.18}$$

Note that λ has to be positive in order that the integrations $\int d\mu(\phi)$ make sense.

The second form in (3.17) shows Z as the partition function of a generalized Ising model, a typical model studied in statistical physics. For $\lambda \to \infty$ the distribution $d\mu(\phi)$ peaks at $\phi^2 = 1$,

$$\frac{\int d\mu(\phi)\, f(\phi)}{\int d\mu(\phi)} \to \frac{\int d\Omega_n\, f(\phi)}{\int d\Omega_n}, \tag{3.19}$$

where $\int d\Omega_n$ is the integral over the unit sphere S^n in n dimensions. In particular, for $n = 1$,

$$\frac{\int d\mu(\phi)\, f(\phi)}{\int d\mu(\phi)} \to \frac{1}{2}[f(1) + f(-1)]. \tag{3.20}$$

Hence, for $n = 1$ and $\lambda \to \infty$ we get precisely the Ising model in d dimensions. For $n = 3$, $d = 3$ the model is called the Heisenberg model for a ferromagnet. The $O(n)$ models on the lattice are therefore also called (generalized) spin models.

3.3 Phase diagram and critical line

The spin model aspect makes it plausible that the models can be in a broken (ferromagnetic) or in a symmetric (paramagnetic) phase, such that in the thermodynamic limit and for zero temperature

$$\langle\phi_x^\alpha\rangle \equiv v^\alpha \neq 0, \quad \kappa > \kappa_c(\lambda), \tag{3.21}$$
$$= 0, \quad \kappa < \kappa_c(\lambda). \tag{3.22}$$

Here $\kappa_c(\lambda)$ is the boundary line between the two phases in the λ–κ plane.

We can give a mean-field estimate of κ_c as follows. Consider a site x. The probability for ϕ_x^α is proportional to $d\mu(\phi_x)\exp[\,2\kappa\phi_x^\alpha\sum_\mu(\phi_{x+\hat\mu}^\alpha + \phi_{x-\hat\mu}^\alpha)\,]$. Assume that we may approximate ϕ^α at the $2d$ neighbors of x by their average value, $\sum_\mu(\phi_{x+\hat\mu}^\alpha + \phi_{x-\hat\mu}^\alpha) \to 2dv^\alpha$. Then the average value of ϕ_x^α can be written as

$$\langle\phi_x^\alpha\rangle = \frac{\int d\mu(\phi)\,\phi^\alpha\exp(4\kappa d\phi^\beta v^\beta)}{\int d\mu(\phi)\,\exp(4\kappa d\phi^\beta v^\beta)}. \tag{3.23}$$

By consistency we should have $\langle\phi_x^\alpha\rangle = v^\alpha$, or

$$v^\alpha = \frac{1}{z(J)}\,\frac{\partial}{\partial J_\alpha}z(J)_{|J=4\kappa dv}, \tag{3.24}$$
$$z(J) = \int d\mu(\phi)\exp(J_\alpha\phi^\alpha). \tag{3.25}$$

The integral $z(J)$ can be calculated analytically in various limits, numerically otherwise. The basics are already illustrated by the Ising case $n=1$, $\lambda=\infty$,

$$z(J) = z(0)\cosh(J), \tag{3.26}$$
$$v = \tanh(4\kappa dv), \quad n=1,\ \lambda=\infty. \tag{3.27}$$

The equation for v can be analyzed graphically, see figure 3.2. As $\kappa \searrow \kappa_c$, evidently $v\to 0$. Then we can expand

$$v = \tanh(4\kappa dv) = 4\kappa dv - \tfrac{1}{3}(4\kappa dv)^3 + \cdots, \tag{3.28}$$
$$\kappa_c = \frac{1}{4d}, \tag{3.29}$$
$$v^2 \propto (\kappa-\kappa_c), \ \ \kappa\searrow\kappa_c. \tag{3.30}$$

Analysis for arbitrary n and λ leads to similar conclusions,

$$z(J) = z(0)\langle 1 + \phi^\alpha J_\alpha + \tfrac{1}{2}\phi^\alpha\phi^\beta J_\alpha J_\beta + \cdots\rangle_1 \tag{3.31}$$
$$= z(0)\left[1 + \frac{1}{2}\frac{\langle\phi^2\rangle_1}{n}J_\alpha J_\alpha + \cdots\right], \tag{3.32}$$

https://doi.org/10.1017/9781009402705.004 Published online by Cambridge University Press

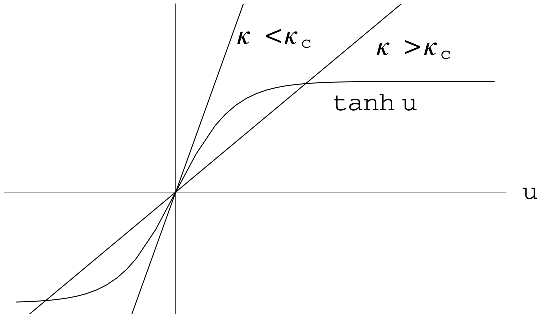

Fig. 3.2. Mean-field equation $u/4d\kappa = \tanh u$, $u = 4d\kappa v$, for $n = 1$, $\lambda = \infty$.

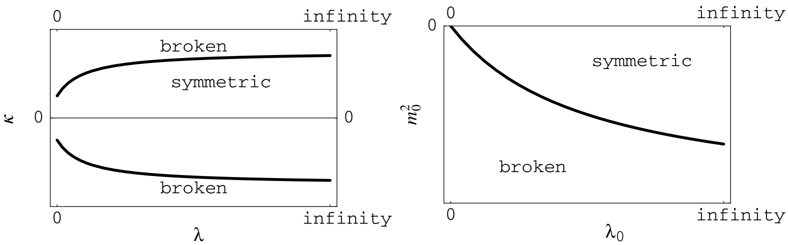

Fig. 3.3. Critical lines in the λ–κ plane and the m_0^2–λ_0 plane (qualitative).

where we used the notation

$$\langle F \rangle_1 = \frac{\int d\mu(\phi)\, F(\phi)}{\int d\mu(\phi)}, \tag{3.33}$$

and

$$\langle \phi^\alpha \phi^\beta \rangle_1 = \delta_{\alpha\beta} \frac{\langle \phi^2 \rangle_1}{n}, \tag{3.34}$$

for the one-site averages. So we find

$$\kappa_c(\lambda) = \frac{n}{4d\langle \phi^2 \rangle_1} = \frac{n}{4d}, \quad \lambda = \infty, \tag{3.35}$$

$$= \frac{1}{2d}, \quad \lambda = 0. \tag{3.36}$$

The behavior $v^2 \propto (\kappa - \kappa_c)$ is typical for a second-order phase transition in the mean-field approximation. The line $\kappa = \kappa_c(\lambda)$ is a critical line in parameter space where a second-order phase transition takes place. Note that in general m_0^2 is negative at the phase boundary

https://doi.org/10.1017/9781009402705.004 Published online by Cambridge University Press

(cf. (3.15) and figure 3.3). The critical exponent β in

$$v \propto (\kappa - \kappa_{\rm c})^{\beta} \tag{3.37}$$

differs in general from the mean-field value $\beta = \frac{1}{2}$. This is the subject of the theory of critical phenomena, and indeed, that theory is crucial for quantum fields. In four dimensions, however, it turns out that there are only small corrections to mean-field behavior.

We have restricted ourselves here to the region $\kappa > 0$. For $\kappa < 0$ the story more or less repeats itself, we then get an antiferromagnetic phase for $\kappa < -\kappa_{\rm c}(\lambda)$. The region with negative κ can be mapped onto the region of positive κ by the transformation $\phi_x^\alpha \to (-1)^{x_1+x_2+\cdots+x_d}\phi_x^\alpha$.

It is important that the phase transition is of second order rather than, for example, of first order. In a second-order transition the correlation length diverges as a critical point is approached. The correlation length ξ can then be interpreted as the physical length scale and, when physical quantities are expressed in terms of ξ, the details on the scale of the lattice distance become irrelevant. The correlation length is defined in terms of the long-distance behavior of the correlation function,

$$G_{xy}^{\alpha\beta} \equiv \langle\phi_x^\alpha\phi_y^\beta\rangle - \langle\phi_x^\alpha\rangle\langle\phi_y^\beta\rangle \tag{3.38}$$

$$\propto |x-y|^{2-d-\eta} e^{-|x-y|/\xi}, \quad |x-y| \to \infty. \tag{3.39}$$

Here ξ may in principle depend on the direction we take $|x-y|$ to infinity, but the point is that it becomes independent of that direction (a lattice detail) as $\xi \to \infty$. In the symmetric phase ξ is independent of α and β. The exponent η is another critical exponent.

The correlation length is the inverse mass gap, the Compton wave length of the lightest particle, in lattice units,

$$\xi = 1/am. \tag{3.40}$$

This can be understood from the spectral representation

$$G_{xy}^{\alpha\beta} = \sum_{\mathbf{p},\gamma\neq 0} \langle 0|\phi_{\mathbf{0}}^\alpha|\mathbf{p}\gamma\rangle\langle\mathbf{p}\gamma|\phi_{\mathbf{0}}^\beta|0\rangle e^{i\mathbf{p}(\mathbf{x}-\mathbf{y})-\omega_{\mathbf{p}\gamma}|x_4-y_4|}, \tag{3.41}$$

where $|0\rangle$ is the ground state (vacuum), $|\mathbf{p}\gamma\rangle$ are states with total momentum $\mathbf{p}$, distinguished by other quantum numbers γ, and $\omega_{\mathbf{p}\gamma} = E_{\mathbf{p},\gamma} - E_0$ is the difference in energy from the ground state. This representation is obtained by writing the path integral in terms of the transfer operator and its eigenstates in the limit of zero temperature,

https://doi.org/10.1017/9781009402705.004 Published online by Cambridge University Press

using translation invariance (cf. problem (viii) in chapter 2). Expression (3.41) is a sum of exponentials $\exp(-\omega t)$, $t = |x_4 - y_4|$. For large t the exponential with smallest ω dominates, $G \propto \exp(-\omega_{\min} t)$, hence $\xi = 1/\omega_{\min}$, with $\omega_{\min} = m$ the minimum energy or mass gap.

In the broken phase we expect Goldstone bosons (section 3.1). If these are made sufficiently heavy by adding an explicit symmetry-breaking term $\sum_x \epsilon\varphi_x^n$ to the action (cf. equation (3.11)), we can expect two mass gaps: m_σ for the components of $G^{\alpha\beta}$ parallel to v^α and m_π for the components perpendicular to v^α. When the explicit symmetry breaking is diminished, $2m_\pi$ becomes less than m_σ and the σ particle becomes unstable, $\sigma \to 2\pi$. Then the large-distance behavior for the σ correlation function is controlled by $2m_\pi$ rather than by the mass m_σ of the unstable particle. Since m_π is expected to be zero in absence of explicit symmetry breaking, the transverse correlation length will be infinite in this case (for infinite volume).

The region near the phase boundary line where $\xi \gg 1$ is called the scaling region. In this region, at large distances $|x - y|$, the correlation function G_{xy} is expected to become a universal scaling function (independent of lattice details, with $1/m$ as the only relevant length scale rather than a).

3.4 Weak-coupling expansion

Expansion of the path-integral expectation value

$$\langle F(\varphi)\rangle = \frac{1}{Z}\int D\varphi\, e^{S(\varphi)} F(\varphi), \tag{3.42}$$

$$S(\varphi) = -\sum_x \left[\frac{1}{2}\partial_\mu\varphi^\alpha\partial_\mu\varphi^\alpha + \frac{1}{2}m_0^2\varphi^2 + \frac{1}{4}\lambda_0(\varphi^2)^2\right], \tag{3.43}$$

in powers of λ_0 leads to Feynman diagrams in terms of the free propagator and vertex functions. For simplicity we shall deal with the symmetric phase, which starts out with $m_0^2 > 0$ in the weak-coupling expansion. The free propagator is given by

$${}^0G_{xy}^{\alpha\beta} = \delta_{\alpha\beta}\sum_p e^{ip(x-y)}\frac{1}{m_0^2 + \sum_\mu(2 - 2\cos p_\mu)}, \tag{3.44}$$

https://doi.org/10.1017/9781009402705.004 Published online by Cambridge University Press

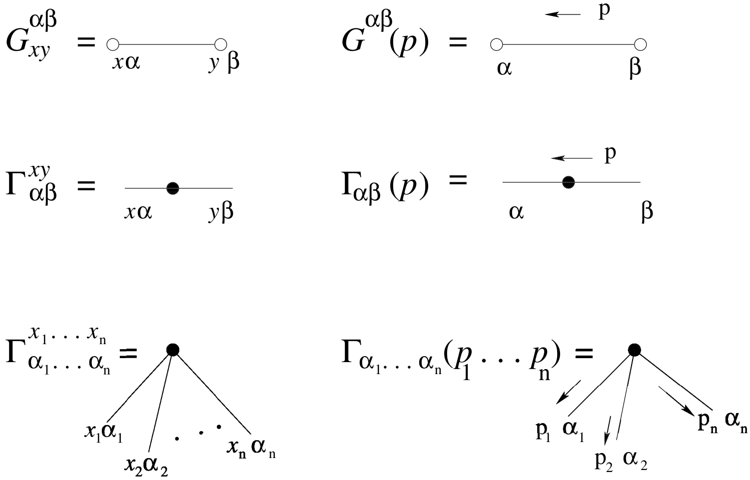

Fig. 3.4. Diagrams for ${}^0G$, ${}^0\Gamma_{(2)}$ and ${}^0\Gamma_{(n)}$. Notice the convention of attaching a small circle at the end of external lines that represent propagators; without this $\circ$ the external line does not represent a propagator.

which is minus the inverse of the free second-order vertex function $\delta_{\alpha\beta}S_{xy}$ (recall (2.99) and (2.108)), which we shall denote here by ${}^0\Gamma_{(2)}$. In momentum space

$$ {}^0\Gamma_{\alpha\beta}(p) = -\delta_{\alpha\beta}\left[m_0^2 + \sum_\mu (2 - 2\cos p_\mu)\right]. \tag{3.45} $$

The bare (i.e. lowest-order) vertex functions ${}^0\Gamma_{(n)}$ are defined by the expansion of the action S around the classical minimum $\varphi^\alpha_x = v^\alpha$,

$$ S(\varphi) = \sum_n \frac{1}{n!}\, {}^0\Gamma^{x_1\cdots x_n}_{\alpha_1\cdots\alpha_n}(\varphi^{\alpha_1}_{x_1} - v^{\alpha_1})\cdots(\varphi^{\alpha_n}_{x_n} - v^{\alpha_n}). \tag{3.46} $$

Since they correspond to a translationally invariant theory, their Fourier transform contains a $\bar{\delta}$ function expressing momentum conservation modulo 2π (cf. (2.90)),

$$ \sum_{x_1\cdots x_n} e^{-ip_1x_1\cdots - ip_nx_n}\, {}^0\Gamma^{x_1\cdots x_n}_{\alpha_1\cdots\alpha_n} = {}^0\Gamma_{\alpha_1\cdots\alpha_n}(p_1\cdots p_n)\,\bar{\delta}_{p_1+\cdots+p_n,0}. \tag{3.47} $$

In the symmetric phase ($v^\alpha = 0$) there is only one interaction vertex

https://doi.org/10.1017/9781009402705.004 Published online by Cambridge University Press

function, the four-point function

$$
\begin{aligned}
{}^0\Gamma^{wxyz}_{\alpha\beta\gamma\delta} &= -2\lambda_0(\delta_{\alpha\beta}\delta_{\gamma\delta} + \delta_{\alpha\gamma}\delta_{\beta\delta} + \delta_{\alpha\delta}\delta_{\beta\gamma})\delta_{wx}\delta_{wy}\delta_{wz}, \\
{}^0\Gamma_{\alpha_1\cdots\alpha_n}(p_1\cdots p_n) &= -2\lambda_0\, s_{\alpha\beta\gamma\delta}, \qquad (3.48)\\
s_{\alpha\beta\gamma\delta} &\equiv \delta_{\alpha\beta}\delta_{\gamma\delta} + \delta_{\alpha\gamma}\delta_{\beta\delta} + \delta_{\alpha\delta}\delta_{\beta\gamma}. \qquad (3.49)
\end{aligned}
$$

The free propagators and vertex functions are illustrated in figure 3.4.

It can be shown that disconnected subdiagrams without external lines ('vacuum bubbles') cancel out between the numerator and the denominator in the above expectation values. The expectation values can be rewritten in terms of vertex functions, which are simpler to study because they have fewer diagrams in a given order in λ_0. The two- and four-point functions can be expressed as

$$
\begin{aligned}
\langle \varphi^{\alpha_1}_{x_1}\varphi^{\alpha_2}_{x_2}\rangle &= G^{\alpha_1\alpha_2}_{x_1x_2} \equiv G^{12}, \qquad (3.50)\\
\langle \varphi^{\alpha_1}_{x_1}\varphi^{\alpha_2}_{x_2}\varphi^{\alpha_3}_{x_3}\varphi^{\alpha_4}_{x_4}\rangle &= G^{12}G^{34} + G^{13}G^{24} + G^{14}G^{23} + G^{1234}, \qquad (3.51)
\end{aligned}
$$

and the vertex functions $\Gamma_{(2)}$ and $\Gamma_{(4)}$ can be identified by writing

$$
\begin{aligned}
G^{12} &= -\Gamma^{-1}_{12}, \qquad (3.52)\\
G^{1234} &= G^{11'}G^{22'}G^{33'}G^{44'}\Gamma_{1'2'3'4'}, \qquad (3.53)
\end{aligned}
$$

where as usual repeated indices are summed. Notice that Γ_{123} is zero in the symmetric phase.

To one-loop order Γ_{12} and Γ_{1234} are given by the connected diagrams in figure 3.5,

$$
\begin{aligned}
\Gamma_{12} &= {}^0\Gamma_{12} + \tfrac{1}{2}\,{}^0\Gamma_{1234}\,{}^0G^{34}, \qquad (3.54)\\
\Gamma_{1234} &= {}^0\Gamma_{1234} + \tfrac{1}{2}\,{}^0\Gamma_{1256}\,{}^0G^{55'}\,{}^0G^{66'}\,{}^0\Gamma_{5'6'34} \\
&\qquad + \text{two permutations}. \qquad (3.55)
\end{aligned}
$$

In momentum space, we have conservation of momentum modulo 2π at each vertex. This may be replaced by ordinary momentum conservation because all functions in momentum space have period 2π anyway. We find for the two-point vertex function

$$
\begin{aligned}
\Gamma_{\alpha_1\alpha_2}(p) &= -(m_0^2 + \hat{p}^2)\delta_{\alpha_1\alpha_2} \\
&\qquad + \frac{1}{2}(-2\lambda_0)s_{\alpha_1\alpha_2\alpha_3\alpha_4}\,\delta_{\alpha_3\alpha_4}\sum_l \frac{1}{m_0^2 + \hat{l}^2} \qquad (3.56)\\
&\equiv -\delta_{\alpha_1\alpha_2}[\,m_0^2 + \hat{p}^2 + \lambda_0(n+2)I(m_0)\,], \qquad (3.57)
\end{aligned}
$$

https://doi.org/10.1017/9781009402705.004 Published online by Cambridge University Press

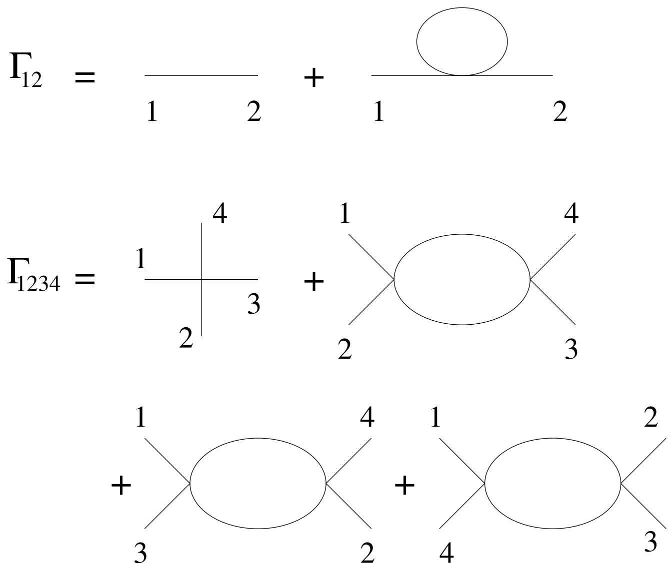

Fig. 3.5. Diagrams for Γ_{12} and Γ_{1234} to one-loop order.

and for the four-point vertex function

$$\begin{aligned}\Gamma_{\alpha_1\alpha_2\alpha_3\alpha_4}(p_1p_2p_3p_4) &= -2\lambda_0 s_{\alpha_1\alpha_2\alpha_3\alpha_4} \\ &\quad + \frac{1}{2}(2\lambda_0)^2 s_{\alpha_1\alpha_2\alpha_5\alpha_6} s_{\alpha_3\alpha_4\alpha_5\alpha_6} \sum_l \frac{1}{m_0^2 + \hat{l}^2} \\ &\quad \times \frac{1}{m_0^2 + 2\sum_\mu (1-\cos(l+p_1+p_2)_\mu)} \\ &\quad + \text{two permutations} \qquad (3.58) \\ &\equiv -2\lambda_0 s_{\alpha_1\alpha_2\alpha_3\alpha_4} + 2\lambda_0^2 t_{\alpha_1\alpha_2\alpha_3\alpha_4} J(m_0, p_1+p_2) \\ &\quad + \text{two permutations.}\end{aligned}$$

Here

$$\hat{l}^2 = 2\sum_\mu (1-\cos l_\mu), \qquad (3.59)$$

and similarly for $\hat{p}^2$, and (using the condensed notation $\delta_{12} = \delta_{\alpha_1\alpha_2}$ etc.)

$$s_{1234} = \delta_{12}\delta_{34} + \delta_{13}\delta_{24} + \delta_{14}\delta_{23}, \qquad (3.60)$$

$$t_{1234} = s_{1256}s_{3456} = \delta_{12}\delta_{34}(n+4) + 2\delta_{13}\delta_{24} + 2\delta_{14}\delta_{23}. \qquad (3.61)$$

https://doi.org/10.1017/9781009402705.004 Published online by Cambridge University Press

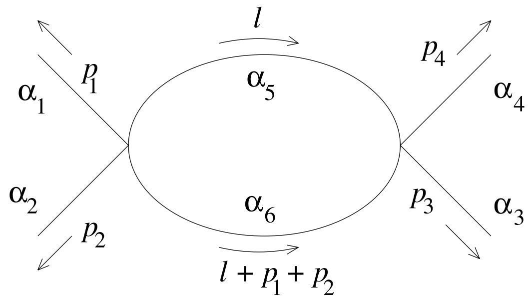

Fig. 3.6. Momentum flow.

The functions I and J are given by

$$I(m_0) = \int_{-\pi}^{\pi} \frac{d^4 l}{(2\pi)^4} \frac{1}{m_0^2 + \hat{l}^2}, \tag{3.62}$$

$$J(m_0, p) = \int_{-\pi}^{\pi} \frac{d^4 l}{(2\pi)^4} \frac{1}{\{m_0^2 + \hat{l}^2\}\{m_0^2 + 2\sum_\mu (1 - \cos(l+p)_\mu)\}}.$$

We assumed an infinite lattice, $\sum_l \to \int d^4 l/(2\pi)^4$. The momentum flow in the second term in (3.58) is illustrated in figure 3.6

We are interested in the scaling forms of I and J. Let us therefore restore the lattice distance a. The functions I and J have dimensions a^{-2} and a^0, respectively. We are interested in $a^{-2} I(am_0)$ and $J(am_0, ap)$, for $a \to 0$. This suggests expanding in powers of a and keeping only terms nonvanishing as $a \to 0$. For I we need terms of order a^0 and a^2, for J only terms of order a^0. Consider first I. A straightforward expansion $1/(a^2 m_0^2 + \hat{l}^2) = \sum_n (-a^2 m_0^2)^n / (\hat{l}^2)^{n+1}$ leads to divergences in the loop integrals at the origin $l = 0$. There are various ways to deal with this situation. Here we shall give just one. Intuitively we know that the region near the origin in momentum space corresponds to continuum physics. Let us split the integration region into a ball round the origin with radius δ and the rest, with $a \ll \delta$. The radius δ is sent to zero, such that, for the integrand in the region $|l| < \delta$, we may use the continuum form l^2 for $\hat{l}^2$. Then

$$I = I_{|l|<\delta} + I_{|l|>\delta}, \tag{3.63}$$

$$I_{|l|<\delta}(am_0) = \int_{|l|<\delta} \frac{d^4 l}{(2\pi)^4} \frac{1}{a^2 m_0^2 + l^2} = \frac{2\pi^2}{(2\pi)^4} \int_0^\delta l^3\, dl\, \frac{1}{a^2 m_0^2 + l^2}$$

https://doi.org/10.1017/9781009402705.004 Published online by Cambridge University Press

$$= \frac{1}{16\pi^2}\left[\delta^2 - a^2m_0^2 \ln\left(\frac{a^2m_0^2+\delta^2}{a^2m_0^2}\right)\right]$$
$$= \frac{1}{16\pi^2}[-a^2m_0^2\ln\delta^2 + a^2m_0^2\ln(a^2m_0^2)] + O(a^4,\delta^2). \tag{3.64}$$

With symbols like $O(a^2)$ we shall mean terms proportional to a^2 or $a^2 \ln a^2$. Note that expressing also l in physical units, $l \to al$, would bring $a^{-2}I_{|l|<\delta}$ into continuum form with a spherical cutoff δ/a. The integral $I_{|l|>\delta}$ can be expanded in a^2 without encountering $\ln(a^2m_0^2)$ terms,

$$I_{|l|>\delta}(am_0) = I_{|l|>\delta}(0) + I'_{|l|>\delta}(0)a^2m_0^2 + O(a^4)$$
$$= I(0) + I'_{|l|>\delta}(0)a^2m_0^2 + O(a^4,\delta^2). \tag{3.65}$$

where $I' \equiv \partial I/\partial(a^2m_0^2)$. Instead, we encounter $\ln\delta^2$ terms in $I'_{|l|>\delta}(0)$. However, these cancel out against the $\ln\delta^2$ term in (3.64) because the complete integral is independent of δ. So we get

$$I(am_0) = C_0 - C_2a^2m_0^2 + \frac{1}{16\pi^2}a^2m_0^2\ln(a^2m_0^2), \tag{3.66}$$
$$C_0 = I(0) = 0.154933\ldots \tag{3.67}$$
$$C_2 = \lim_{\delta\to 0}\left[\int_{-\pi,|l|>\delta}^{\pi} \frac{d^4l}{(2\pi)^4}\frac{1}{(\hat{l}^2)^2} + \frac{1}{16\pi^2}\ln\delta^2\right] \tag{3.68}$$
$$= 0.0303457\ldots. \tag{3.69}$$

The function J can be evaluated in similar fashion. We need $J(am_0, ap)$ for $a \to 0$. For $a = 0$ the integral for J is logarithmically divergent at the origin. To deal with this we use the same procedure,

$$J = J_{|l|<\delta} + J_{|l|>\delta}, \tag{3.70}$$
$$J_{|l|<\delta} = \int_{|l|<\delta}\frac{d^4l}{(2\pi)^4}\frac{1}{[a^2m_0^2+l^2][a^2m_0^2+(l+ap)^2]}, \tag{3.71}$$
$$J_{|l|>\delta} = \int_{\pi,|l|>\delta}^{-\pi}\frac{d^4l}{(2\pi)^4}\frac{1}{(\hat{l}^2)^2} + O(a^2) \tag{3.72}$$

($J_{|l|>\delta}$ can be expanded in powers of a, the term linear in a vanishes). With the help of the identity

$$\frac{1}{[a^2m_0^2+l^2][a^2m_0^2+(l+ap)^2]}$$
$$= \int_0^1 dx\,\frac{1}{\{x[a^2m_0^2+l^2]+(1-x)[a^2m_0^2+(l+ap)^2]\}^2} \tag{3.73}$$

https://doi.org/10.1017/9781009402705.004 Published online by Cambridge University Press

and the transformation of variable $l' = l + (1-x)ap$ we get for the inner-region integral

$$J_{|l|<\delta} = \int_0^1 dx \int_D \frac{d^4 l'}{(2\pi)^4} \frac{1}{[a^2 m_0^2 + l'^2 + x(1-x)a^2 p^2]^2}. \tag{3.74}$$

Here the domain of integration D is obtained from the ball with radius δ by shifting it over $(1-x)ap$. Replacing D by the original ball with radius δ leads to an error of order a, which may be neglected. (The difference between the two integration regions has a volume $O(ap\delta^3)$, the integrand is $O(\delta^{-4})$.) Then

$$\begin{aligned} J_{|l|<\delta} &= \int_0^1 dx \, \frac{2\pi^2}{(2\pi)^4} \int_0^\delta l^3 \, dl \, \frac{1}{[a^2 m_0^2 + l^2 + x(1-x)a^2 p^2]^2} \\ &= \frac{1}{16\pi^2} \int_0^1 dx \left[\ln(a^2\Delta + \delta^2) - \ln(a^2\Delta) - \frac{\delta^2}{a^2\Delta + \delta^2} \right] \\ &= \frac{1}{16\pi^2} \left[\ln \delta^2 - \int_0^1 dx \, \ln(a^2\Delta) - 1 \right] + O(a^2), \end{aligned} \tag{3.75}$$

$$\Delta \equiv m^2 + x(1-x)p^2. \tag{3.76}$$

Combining the term $\ln \delta^2/16\pi^2$ with $J_{|l|>\delta}$ as in (3.68) we get

$$J(am_0, ap) = -\frac{1}{16\pi^2} \int_0^1 dx \, \ln[\, a^2(m_0^2 + x(1-x)p^2)] + C_2 - \frac{1}{16\pi^2} + O(a^2). \tag{3.77}$$

(We expect errors $O(a^2)$, i.e. not $O(a)$: a will appear together with the external momentum as ap_μ or as $a^2 m_0^2$, and there will not be odd powers of p_μ because of cubic symmetry, including reflections.)

Summarizing, we have obtained the following continuum forms for the vertex functions (in physical units):

$$\Gamma_{\alpha\beta}(p) = -\delta_{\alpha\beta} \left\{ m_0^2 + p^2 + \lambda_0(n+2) \left[\frac{C_0}{a^2} - C_2 m_0^2 + \frac{1}{16\pi^2} m_0^2 \ln(a^2 m_0^2) \right] \right\}, \tag{3.78}$$

$$\begin{aligned} \Gamma_{\alpha_1\alpha_2\alpha_3\alpha_4}(p_1 p_2 p_3 p_4) = &-2\lambda_0 s_{\alpha_1\alpha_2\alpha_3\alpha_4} \\ &+ 2\lambda_0^2 t_{\alpha_1\alpha_2\alpha_3\alpha_4} \left\{ C_2 - \frac{1}{16\pi^2} - \frac{1}{16\pi^2} \right. \\ &\left. \times \int_0^1 dx \, \ln[a^2(m_0^2 + x(1-x)(p_1+p_2)^2)] \right\} \\ &+ \text{two permutations}, \end{aligned} \tag{3.79}$$

https://doi.org/10.1017/9781009402705.004 Published online by Cambridge University Press

We see that $\Gamma_{(2)}$ and $\Gamma_{(4)}$ are, respectively, quadratically and logarithmically divergent as $a \to 0$.

3.5 Renormalization

Perturbative renormalization theory tells us that, when we rescale the correlation functions $G^{(n)}$ by a suitable factor $Z^{-n/2}$ and express them in terms of a suitable renormalized mass parameter $m_{\rm R}$ and renormalized coupling constant $\lambda_{\rm R}$, the result is finite as $a \to 0$. The renormalized $G_{\rm R}^{(n)} = Z^{-n/2}G^{(n)}$ are the correlation functions of renormalized fields $\varphi_{\rm R} = Z^{-1/2}\varphi$. From (3.53) we see that the renormalized vertex functions are then given by

$$\Gamma^{\rm R}_{(n)} = Z^{n/2}\Gamma_{(n)}. \tag{3.80}$$

The wave function renormalization constant Z and the renormalized mass parameter $m_{\rm R}$ may be defined by the first two terms of the expansion

$$\Gamma_{\alpha\beta}(p) = -Z^{-1}(m_{\rm R}^2 + p^2 + O(p^4))\delta_{\alpha\beta}. \tag{3.81}$$

Since the one-loop diagram for $\Gamma_{(2)}$ is momentum independent, the order λ contribution to Z vanishes in the $O(n)$ model,

$$Z = 1 + O(\lambda^2). \tag{3.82}$$

For $m_{\rm R}$ we find from (3.78)

$$m_{\rm R}^2 = m_0^2 + \lambda_0(n+2)\left[C_0 a^{-2} - C_2 m_0^2 + \frac{1}{16\pi^2} m_0^2 \ln(a^2 m_0^2)\right]. \tag{3.83}$$

A renormalized coupling constant $\lambda_{\rm R}$ may be defined in terms of $\Gamma_{(4)}$ at zero momentum, by writing

$$\Gamma^{\rm R}_{\alpha_1\alpha_2\alpha_3\alpha_4}(0,0,0,0) = -2\lambda_{\rm R}\, s_{\alpha_1\alpha_2\alpha_3\alpha_4}. \tag{3.84}$$

From the result (3.79) for the four-point function, using (3.82) and

$$t_{1234} + t_{1324} + t_{1423} = (n+8)s_{1234}, \tag{3.85}$$

we find

$$\lambda_{\rm R} = \lambda_0 + \lambda_0^2 \frac{n+8}{16\pi^2}[\ln(a^2 m_0^2) + c], \tag{3.86}$$

$$c = -\frac{16\pi^2}{n+8}\left(C_2 - \frac{1}{16\pi^2}\right). \tag{3.87}$$

https://doi.org/10.1017/9781009402705.004 Published online by Cambridge University Press

To express the correlation functions in terms of m_{R} and λ_{R} we consider λ_{R} as an expansion parameter and invert (3.83), (3.86),

$$\begin{aligned} m_0^2 = m_{\mathrm{R}}^2 - \lambda_{\mathrm{R}}(n+2)\left[C_0 a^{-2} - C_2 m_{\mathrm{R}}^2 + \frac{1}{16\pi^2} m_{\mathrm{R}}^2 \ln(a^2 m_{\mathrm{R}}^2)\right] \\ + O(\lambda_{\mathrm{R}}^2), \end{aligned} \tag{3.88}$$

$$\lambda_0 = \lambda_{\mathrm{R}} - \lambda_{\mathrm{R}}^2 \frac{n+8}{16\pi^2}[\ln(a^2 m_{\mathrm{R}}^2) + c] + O(\lambda_{\mathrm{R}}^3). \tag{3.89}$$

Inserting these relations into (3.78), (3.79) gives the renormalized vertex functions

$$\Gamma^{\mathrm{R}}_{\alpha\beta}(p) = -\delta_{\alpha\beta}(m_{\mathrm{R}}^2 + p^2) + O(\lambda_{\mathrm{R}}^2), \tag{3.90}$$

$$\begin{aligned} \Gamma^{\mathrm{R}}_{\alpha_1\alpha_2\alpha_3\alpha_4}(p_1 p_2 p_3 p_4) = & -2\lambda_{\mathrm{R}} s_{\alpha_1\alpha_2\alpha_3\alpha_4} - 2\lambda_{\mathrm{R}}^2 t_{\alpha_1\alpha_2\alpha_3\alpha_4} \\ & \times \frac{1}{16\pi^2}\int_0^1 dx\, \ln\left(\frac{m_{\mathrm{R}}^2 + x(1-x)(p_1+p_2)^2}{m_{\mathrm{R}}^2}\right) \\ & + \text{two permutations} + O(\lambda_{\mathrm{R}}^3), \end{aligned} \tag{3.91}$$

which are indeed independent of the lattice spacing a. Notice that the constants C_0, C_1 and C_2 are absent: all reference to the lattice has disappeared from the renormalized vertex functions.

To this order the mass m of the particles is equal to m_{R}. The mass m is given by the value of $-p^2$ where $\Gamma_{(2)}$ is zero and $G^{(2)}$ has a pole. In higher orders the mass m will be different from the renormalized mass parameter m_{R}: $m = m_{\mathrm{R}}(1 + O(\lambda_{\mathrm{R}}^2))$.

The $O(n)$ tensor structure in (3.84) is the general form of $\Gamma_{(4)}$ at a symmetry point where $(p_1+p_2)^2 = (p_1+p_3)^2 = (p_1+p_4)^2 \equiv \mu^2$. We can therefore also define a 'running renormalized coupling' $\bar{\lambda}(\mu)$ at momentum scale μ by

$$\Gamma^{\mathrm{R}}_{\alpha_1\alpha_2\alpha_3\alpha_4}(p_1 p_2 p_3 p_4) = -2\bar{\lambda}(\mu) s_{\alpha_1\alpha_2\alpha_3\alpha_4}, \quad \text{symmetry point}\, \mu, \tag{3.92}$$

which gives

$$\bar{\lambda}(\mu) = \lambda_0 + \lambda_0^2 \frac{n+8}{16\pi^2}\left\{\int_0^1 dx\, \ln[a^2 m_0^2 + x(1-x)a^2\mu^2] + c\right\}. \tag{3.93}$$

Expressing the running coupling in terms of λ_{R} and m_{R} leads to

$$\begin{aligned} \bar{\lambda}(\mu) &= \lambda_{\mathrm{R}} + \lambda_{\mathrm{R}}^2 \frac{n+8}{16\pi^2}\int_0^1 dx \ln[1 + x(1-x)\mu^2/m_{\mathrm{R}}^2] + O(\lambda_{\mathrm{R}}^3) \\ &= \lambda_{\mathrm{R}}, \qquad \mu = 0, && (3.94) \\ &\approx \lambda_{\mathrm{R}} + \lambda_{\mathrm{R}}^2 \frac{n+8}{16\pi^2}[\ln(\mu^2/m_{\mathrm{R}}^2) - 2], \quad \mu^2 \gg m_{\mathrm{R}}^2. && (3.95) \end{aligned}$$

The running coupling indicates the strength of the interactions at momentum scale μ. Expressing the vertex function (3.91) in terms of this running coupling shows that, at large momenta, terms of the type $\lambda_{\rm R}^2 \ln[(p_1+p_2)^2/m_{\rm R}^2]$ are replaced by $\bar{\lambda}^2(\mu)\ln[(p_1+p_2)^2/\mu^2]$. So, on choosing μ^2 equal to values of $(p_i+p_j)^2$ that typically occur in a given situation, the logarithms are generically not large and the strength of the four-point vertex on this momentum scale is expressed by $\bar{\lambda}(\mu)$.

3.6 Renormalization-group beta functions

The renormalized quantities do not depend explicitly on the lattice distance, all dependence on a is absorbed by the relations between m_0, λ_0 and $m_{\rm R}$, $\lambda_{\rm R}$. Thus it seems that we can take the continuum limit $a \to 0$ in the renormalized quantities. Changing a while keeping $m_{\rm R}$ and $\lambda_{\rm R}$ fixed implies that m_0 and λ_0 must be chosen to depend on a, as given by (3.88) and (3.89). We see that $a^2 m_0^2$ decreases and becomes negative as a decreases, even in the symmetric phase. This we found earlier in the mean-field approximation. However, the bare λ_0 increases as a decreases and beyond a certain value we can no longer trust perturbation theory in λ_0. Neither can we trust (3.89) if a becomes too small, since then the coefficient of $\lambda_{\rm R}^2$ blows up.

Let us look at the problem in another way. Consider what happens to $\lambda_{\rm R}$ as we approach the phase boundary at fixed λ_0. In (3.86) we may replace to this order m_0 by $m_{\rm R}$,

$$\lambda_{\rm R} = \lambda_0 + \lambda_0^2 \frac{n+8}{16\pi^2}[\ln(a^2 m_{\rm R}^2) + c] + O(\lambda_0^3). \tag{3.96}$$

We see that $\lambda_{\rm R}$ decreases as a decreases, but when the logarithm becomes too large the perturbative relation breaks down. We can extract more information by differentiating with respect to a and writing the result in terms of $\lambda_{\rm R}$,

$$\beta_{\rm R}(\lambda_{\rm R}) = \left[a\,\frac{\partial \lambda_{\rm R}}{\partial a}\right]_{\lambda_0} = \left[a m_{\rm R}\,\frac{\partial \lambda_{\rm R}}{\partial a m_{\rm R}}\right]_{\lambda_0}$$

$$= \beta_1 \lambda_0^2 + O(\lambda_0^3) \tag{3.97}$$

$$= \beta_1 \lambda_{\rm R}^2 + \beta_2 \lambda_{\rm R}^3 + \cdots, \tag{3.98}$$

$$\beta_1 = \frac{n+8}{8\pi^2}. \tag{3.99}$$

The function $\beta_{\rm R}(\lambda_{\rm R})$ is one of the renormalization-group functions introduced by Callan and by Symanzik. For a clear derivation of the

https://doi.org/10.1017/9781009402705.004 Published online by Cambridge University Press

Callan–Symanzik equations in our context see [20]. They are dimensionless functions which may be expressed in terms of renormalized vertex functions and are given by renormalized perturbation theory as a series $\sum_k \beta_k \lambda_{\rm R}^k$. This means that the higher-order terms of the form $\lambda_0^k[\ln(am_{\rm R})]^l$ can be rearranged in terms of powers of $\lambda_{\rm R}$ with coefficients that do not depend any more on $\ln(am_{\rm R})$. This is the justification for rewriting (3.97) in terms of $\lambda_{\rm R}$.

Integration of $\partial\lambda_{\rm R}/\partial t = -\beta_1\lambda_{\rm R}^2$ gives

$$\lambda_{\rm R} = \frac{\lambda_1}{1+\lambda_1\beta_1 t}, \quad t \equiv -[\ln(am_{\rm R}) + c/2], \tag{3.100}$$

where λ_1 is an integration constant, $\lambda_1 = \lambda_0 + O(\lambda_0^2)$. As $a \to 0$, $t \to \infty$ and we see that $\lambda_{\rm R}$ approaches zero. The approximation of using only the lowest-order approximation to the beta function is therefore self-consistent.

Let us try the beta-function trick on λ_0 to see whether we can determine how it depends on a if we keep $\lambda_{\rm R}$ fixed. From (3.89) we find

$$\left[a\,\frac{\partial\lambda_0}{\partial a}\right]_{\lambda_{\rm R}} \equiv -\beta_0(\lambda_0) = -\beta_1\lambda_0^2 + \cdots. \tag{3.101}$$

Note the change of sign compared with (3.98). Integrating this equation gives

$$\lambda_0 = \frac{\lambda_2}{1-\lambda_2\beta_1 t}, \tag{3.102}$$

where $\lambda_2 = \lambda_{\rm R} + O(\lambda_{\rm R}^2)$. We see that λ_0 blows up at the 'Landau pole' $t = 1/\lambda_2\beta_1$, but, of course, before reaching this value the first-order approximation to $\beta_0(\lambda_0)$ breaks down.

Consider next the beta function $\bar\beta(\bar\lambda)$ for the running coupling $\bar\lambda(\mu)$ on momentum scale μ. From (3.95) we see that, for large $\mu \gg m_{\rm R}$,

$$\left[\mu\,\frac{\partial\bar\lambda(\mu)}{\partial\mu}\right]_{\lambda_{\rm R},m_{\rm R}} \equiv \bar\beta(\bar\lambda) = \beta_1\bar\lambda^2 + \cdots, \quad \mu \gg m_{\rm R}, \tag{3.103}$$

again with the same universal coefficient for the first-order term in its expansion. The solution is similar to that for λ_0,

$$\bar\lambda = \frac{\lambda_3}{1-\lambda_3\beta_1\ln(\mu/m_{\rm R})}. \tag{3.104}$$

The effective coupling $\bar\lambda$ increases with momentum scale μ. To see if it can become arbitrarily large we need to go beyond the weak-coupling expansion.

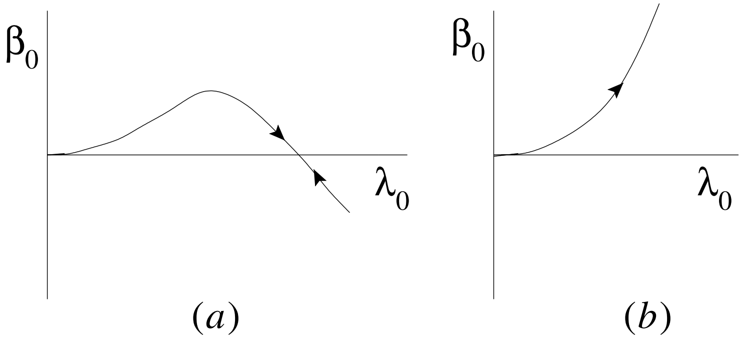

Fig. 3.7. Two possible shapes of $\beta_0(\lambda_0)$. The arrows denote the flow of λ_0 for increasing $t = -\ln(am_{\rm R}) + \text{constant}$.

We end this section by speculating about different shapes of the beta function β_0 for the bare coupling constant. Two typical possibilities are shown in figure 3.7. In case (a) there is a fixed point λ^* that attracts the flow of λ_0 for increasing 'time' t. Near λ^* we can linearize

$$\frac{\partial \lambda_0}{\partial t} = -A(\lambda_0 - \lambda^*), \tag{3.105}$$

$$\lambda_0 - \lambda^* = C \exp(-At), \quad t \to \infty, \tag{3.106}$$

where C is an integration constant. The large-t behavior can be rewritten in the form

$$\xi = \frac{1}{am_{\rm R}} \propto (\lambda^* - \lambda_0)^{-\nu}, \quad \nu = 1/A, \tag{3.107}$$

which shows that the critical exponent ν is determined by the slope of the beta function at the fixed point. Since t can go to infinity without a problem, a continuum *limit* $a \to 0$ is possible for case (a).

In case (b) the beta function does not have a zero, apart from the origin $\lambda_0 = 0$. Supposing a behavior

$$\frac{\partial \lambda_0}{\partial t} = A\lambda_0^\alpha, \quad \lambda_0 \to \infty,\, \alpha > 0,\, A > 0, \tag{3.108}$$

leads to the asymptotic solution

$$\lambda_0^{-(\alpha-1)} = -A(\alpha - 1)(t - t_1), \tag{3.109}$$

where we assumed $\alpha > 1$. In this case λ_0 becomes infinite in a finite 'time' $t = t_1$. Since $\lambda_0 = \infty$ is the largest value λ_0 can take, t cannot go beyond t_1, a cannot go to zero and a continuum *limit* is not possible.

https://doi.org/10.1017/9781009402705.004 Published online by Cambridge University Press

A similar discussion can be given for the running coupling $\bar{\lambda}$. Cases (a) and (b) also illustrate possible behaviors of the running coupling for large momentum scales μ. In case (a) the running coupling approaches λ^* as $\mu \to \infty$, whereas in case (b) $\bar{\lambda}$ goes to infinity on some large but finite momentum scale μ_1.

A fixed point like λ^* is called ultraviolet stable as it attracts the running coupling when $\mu \to \infty$, while the fixed point at the origin is called infrared stable as it attracts the running coupling for $\mu \to 0$. Case (a) is like the situation in three Euclidean dimensions (with a reflection about the horizontal axis), whereas we shall see in the following that in four dimensions the situation is like case (b).

The main conclusion in this section is that $\lambda_{\mathrm{R}} \to 0$ as we approach the phase boundary at fixed sufficiently small λ_0. To see whether we can avoid a noninteracting theory in the continuum *limit*, we need to be able to investigate large λ_0. This can be done with the hopping expansion and with numerical simulations.

3.7 Hopping expansion

Consider the partition function in the form

$$Z = \int D\mu(\phi) \prod_{x\mu} \exp(2\kappa \phi_x^\alpha \phi_{x+\hat{\mu}}^\alpha), \tag{3.110}$$

where $D\mu(\phi) = \prod_x d\mu(\phi_x)$ is the product of one-site measures defined in (3.18). Expansion in κ (hopping expansion) leads to products of one-site integrals of the form

$$\int D\mu(\phi) \equiv Z_0 = \left(\int d\mu(\phi)\right)^{\#\,\mathrm{sites}}, \tag{3.111}$$

$$\int D\mu(\phi)\, \phi_x^\alpha \phi_y^\beta = \delta_{xy} Z_0 \langle \phi^\alpha \phi^\beta \rangle_1, \tag{3.112}$$

$$\int D\mu(\phi)\, \phi_x^\alpha \phi_y^\beta \phi_z^\gamma = 0, \tag{3.113}$$

$$\int D\mu(\phi)\, \phi_x^\alpha \phi_x^\beta \phi_x^\gamma \phi_x^\delta = Z_0 \langle \phi^\alpha \phi^\beta \phi^\gamma \phi^\delta \rangle_1, \tag{3.114}$$

etc., where # sites is the total number of lattice sites. Odd powers of ϕ vanish in the one-site average

$$\langle F \rangle_1 = \int d\mu(\phi)\, F(\phi) \Big/ \int d\mu(\phi). \tag{3.115}$$

https://doi.org/10.1017/9781009402705.004 Published online by Cambridge University Press

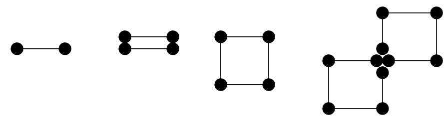

Fig. 3.8. Diagrams in the expansion of $\exp(2\kappa \sum_{x\mu} \phi_x^\alpha \phi_{x+\hat{\mu}}^\alpha)$.

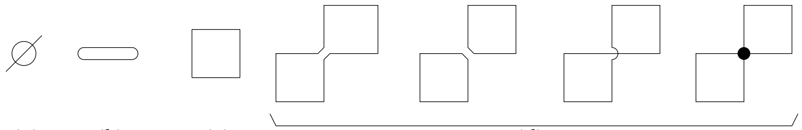

Fig. 3.9. The diagrams of figure 3.8 after integration over ϕ. The fat dot denotes the four-point vertex γ_4.

Before integration over ϕ, each term in the expansion can be represented by a dimer diagram 'on the lattice', as illustrated in figure 3.8. The dots indicate the fields ϕ. The integration over ϕ leads to diagrams as shown in figure 3.9.

The one-site integrals can be treated as a mini field theory, with propagators $g^{\alpha\beta}$ and vertex functions $\gamma_{\alpha_1\cdots\alpha_4}$, $\gamma_{\alpha_1\cdots\alpha_6}$, ... For instance, $\gamma_{\alpha\beta\gamma\delta}$ can be defined by

$$\langle \phi^\alpha \phi^\beta \rangle_1 = g^{\alpha\beta}, \tag{3.116}$$

$$\langle \phi^\alpha \phi^\beta \phi^\gamma \phi^\delta \rangle_1 = g^{\alpha\beta} g^{\gamma\delta} + g^{\alpha\gamma} g^{\beta\delta} + g^{\alpha\delta} g^{\beta\gamma} + g^{\alpha\beta\gamma\delta}, \tag{3.117}$$

$$g^{\alpha\beta\gamma\delta} = g^{\alpha\alpha'} g^{\beta\beta'} g^{\gamma\gamma'} g^{\delta\delta'} \gamma_{\alpha'\beta'\gamma'\delta'}, \tag{3.118}$$

analogously to (3.53). By $O(n)$ symmetry we have

$$g^{\alpha\beta} = \delta_{\alpha\beta}\, g, \quad g = \frac{\langle \phi^2 \rangle_1}{n}, \tag{3.119}$$

$$g^{\alpha\beta\gamma\delta} = s_{\alpha\beta\delta\gamma} \frac{\langle (\phi^2)^2 \rangle_1}{n^2 + 2n}, \tag{3.120}$$

$$\gamma_{\alpha\beta\gamma\delta} = s_{\alpha\beta\delta\gamma}\, \gamma_4, \quad \gamma_4 = \frac{n^3}{n+2} \frac{\langle (\phi^2)^2 \rangle_1}{\langle \phi^2 \rangle_1^4} - \frac{n^2}{\langle \phi^2 \rangle_1^2}, \tag{3.121}$$

where $s_{\alpha\beta\delta\gamma} = \delta_{\alpha\beta}\delta_{\gamma\delta} + \cdots$ has been defined in (3.49). For small λ, $\gamma_4 \propto \lambda$, whereas for $\lambda \to \infty$, $\gamma_4 \to -2n^4/(n+2)$.

As usual, one expects that disconnected diagrams cancel out in expressions for the vertex functions, and that the two-point function, $G_{xy}^{\alpha\beta} = \langle \phi_x^\alpha \phi_y^\beta \rangle$, can be expressed as a sum of connected diagrams. It

https://doi.org/10.1017/9781009402705.004 Published online by Cambridge University Press

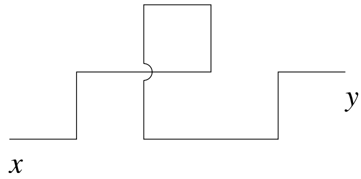

Fig. 3.10. Random-walk contribution to the propagator.

is instructive to make an approximation for the two-point function in which the vertex functions $\gamma_{(4)}$, $\gamma_{(6)}$, ..., are neglected at first. This leads to the random-walk approximation

$$G_{xy}^{\alpha\beta} = \delta_{\alpha\beta} \sum_{L=0}^{\infty} (2\kappa)^{\mathrm{L}} g^{L+1} (H^{\mathrm{L}})_{xy} + \text{'interactions'}, \tag{3.122}$$

illustrated in figure 3.10. Here 'interactions' denote the neglected contributions proportional to $\gamma_{(4)}$, $\gamma_{(6)}$, ..., and we introduced the hopping matrix

$$H_{uv} = \sum_{\mu} (\delta_{u+\hat{\mu}-v,0} + \delta_{v+\hat{\mu}-u,0}). \tag{3.123}$$

Applying this matrix e.g. to the vector $\delta_{v,x}$ gives a non-zero answer only for u's that are nearest neighbors of x, i.e. all sites that can be reached from x in 'one step'. Applying H once more corresponds to making one more step in all possible directions, etc. In this way a random walk is built up by successive application of H. Each link in the expansion contributes a factor 2κ, and each site a factor g. In momentum space we get

$$G_{xy}^{\alpha\beta} = \delta_{\alpha\beta} \int_{-\pi}^{\pi} \frac{d^4p}{(2\pi)^4} e^{ip(x-y)} g \sum_{\mathrm{L}} (2\kappa g)^{\mathrm{L}} H(p)^{\mathrm{L}} \tag{3.124}$$

$$= \delta_{\alpha\beta} \int_{-\pi}^{\pi} \frac{d^4p}{(2\pi)^4} e^{ip(x-y)} \frac{g}{1 - 2\kappa g H(p)}, \tag{3.125}$$

where

$$H(p) = \sum_{x} e^{-ipx} H_{x,0} = \sum_{\mu} 2\cos p_{\mu}. \tag{3.126}$$

In the random-walk approximation the two-point correlation function has the free-field form. For small momenta we identify the mass param-

https://doi.org/10.1017/9781009402705.004 Published online by Cambridge University Press

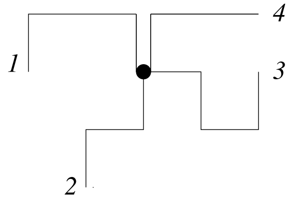

Fig. 3.11. Four random walks correlated by the one site γ_4.

eter $m_{\rm R}$ and the wavefunction-renormalization constant Z_ϕ,

$$G^{\alpha\beta}(p) = \delta_{\alpha\beta}\frac{Z_\phi}{m_{\rm R}^2 + p^2 + O(p^4)}, \tag{3.127}$$

$$Z_\phi = (2\kappa)^{-1}, \quad m_{\rm R}^2 = (2g\kappa)^{-1} - 2d. \tag{3.128}$$

This Z_ϕ corresponds to $Z_\varphi = 1$ (cf. (3.15)). When $m_{\rm R} \to 0$ we enter the scaling region. In the random-walk approximation this occurs at $\kappa = \kappa_{\rm c} = 1/4gd$, which is the mean-field value (3.36). This is not so surprising as the mean-field approximation is good for $d \to \infty$, when also the random-walk approximation is expected to be good, because the chance of self-intersections in the walk, where $\gamma_{(4)}, \gamma_{(6)}, \ldots$ come into play, goes to zero. Notice that $\kappa_{\rm c}$ is also the radius of convergence of the expansion (3.124).

Within the random-walk approximation we have the estimate for the renormalized coupling (cf. (3.80)) as illustrated in figure 3.11,

$$-2\lambda_{\rm R} = Z^2\gamma_4 = \frac{\gamma_4}{4\kappa_{\rm c}^2}, \tag{3.129}$$

$$\lambda_{\rm R} \to \lambda_0, \qquad \lambda \to 0, \tag{3.130}$$

$$\to \left(\frac{2d}{n}\right)^2 \frac{n^2}{n+2} = \frac{32}{3}, \quad \lambda \to \infty,\ d = 4,\ n = 4. \tag{3.131}$$

This indicates already that $\lambda_{\rm R}$ is not infinite at $\lambda = \infty$.

The partition function and expectation values can be expressed as a systematic expansion in κ. This is called the hopping expansion because the random-walk picture suggests propagation of particles by ‘hopping’ from one site to the next. By the analogy of κ with the inverse temperature in the Ising model, the expansion is known in statistical physics as the high-temperature expansion, or, with increasing sophistication, the linked-cluster expansion. Using computers to help with the algebra, the expansion can be carried out to high orders (see e.g. [22] and references therein).

A good property of the hopping expansion is that it has a non-zero radius of convergence, for any fixed $\lambda \in (0, \infty)$. This is in contrast to the weak-coupling expansion, which is an asymptotic expansion (as is typical for saddle-point expansions) with zero radius of convergence (see for example [13]). An expansion $f(x) = \sum_{k=0}^{\infty} f_k x^k$ is called asymptotic if

$$\left| f(x) - \sum_{k=0}^{N} f_k x^k \right| = O(x^{N+1}). \tag{3.132}$$

For fixed finite N the sum gives an accurate approximation to $f(x)$, for sufficiently small x. The expansion need not converge as $N \to \infty$ and for a given x there is an optimum N beyond which the approximation becomes worse.

3.8 Lüscher–Weisz solution

Using the hopping expansion in combination with the Callan–Symanzik renormalization-group equations, Lüscher and Weisz showed how the $O(n)$ models in four dimensions can be solved to a good approximation [20, 21, 22, 23]. The coefficients of the hopping series were calculated to 14th order and the Callan–Symanzik beta functions were used to three-loop order. The cases $n = 1$ [20, 21] and $n = 4$ [23] were worked out in detail. The interested reader is urged to study these lucid papers which contain a lot of information on field theory. We shall review the highlights for the $O(4)$ model.

The critical $\kappa_{\rm c}(\lambda)$ is estimated from the radius of convergence of the hopping expansion to be monotonically increasing from $\kappa_{\rm c} = \frac{1}{8}$ at $\lambda = 0$ to $\kappa_{\rm c} = 0.304\,11(6)$ at $\lambda = \infty$. An important aspect of the results is the carefully estimated errors in various quantities. For simplicity, we shall not quote the errors anymore in the following. Along the line $\kappa = 0.98\,\kappa_{\rm c}$ in the κ–λ plane the hopping expansion still converges well, with the mass parameter $m_{\rm R}$ decreasing from 0.40 to 0.28 and the renormalized coupling $\lambda_{\rm R}$ increasing from 0 to 3.2 as λ increases from 0 to ∞. At a slightly smaller $\kappa < \kappa_{\rm c}$ such that $m_{\rm R} = 0.5$, $\lambda_{\rm R} = 4.3$ for $\lambda = \infty$.

Remarkably, $\lambda_{\rm R} = 3.2$ may be considered as relatively weak coupling. Let us rewrite the beta function

$$m_{\rm R} \frac{\partial \lambda_{\rm R}}{\partial m_{\rm R}} = \beta_{\rm R}(\lambda_{\rm R}) = \beta_1 \lambda_{\rm R}^2 + \beta_2 \lambda_{\rm R}^3 + \cdots, \tag{3.133}$$

https://doi.org/10.1017/9781009402705.004 Published online by Cambridge University Press

in terms of a natural variable $\tilde{\lambda} \equiv \beta_1 \lambda_{\mathrm{R}}$,

$$m_{\mathrm{R}} \frac{\partial \tilde{\lambda}}{\partial m_{\mathrm{R}}} = \tilde{\lambda}^2 + \frac{\beta_2}{\beta_1^2} \tilde{\lambda}^3 + \cdots. \tag{3.134}$$

The results

$$\beta_1 = \frac{n+8}{8\pi^2}, \quad \beta_2 = -\frac{9n+42}{(8\pi^2)^2}, \tag{3.135}$$

give $\beta_2/\beta_1^2 \approx -0.54$. Then $\lambda_{\mathrm{R}} = 3.2$ means $\tilde{\lambda} \approx 0.41$ and the two-loop term in (3.134) is only about 20% of the one-loop term. This indicates that renormalized perturbation theory may be applicable for these couplings. The next (three-loop) term in the series is again positive and Lüscher and Weisz reason that the true beta function in this coupling region may be between the two- and three-loop values.

A basic assumption made in order to proceed is that renormalized perturbation theory is valid for sufficiently small λ_{R}, even if the bare λ is infinite. This may seem daring if one thinks of deriving renormalized perturbation theory from the bare weak-coupling expansion. However, it appears natural from the point of view of Wilson's renormalization theory in terms of an effective action with an effective cutoff, or from the point of view of effective actions, or Schwinger's Source Theory, which uses unitarity to obtain higher-order approximations in an expansion in a physical coupling parameter (e.g. λ_{R}).

Using the beta function calculated in renormalized perturbation theory, Lüscher and Weisz integrate the Callan–Symanzik equations toward the critical point $m_{\mathrm{R}} = 0$. (The variable κ is traded for m_{R}.) As we have seen in (3.100) this leads to the conclusion that the renormalized coupling vanishes at the phase boundary, which is thus established even for bare coupling $\lambda = \infty$ (!).

The integration is done numerically, using (3.133). Sufficiently deep in the scaling region we may integrate by expansion,

$$\frac{\partial \lambda_{\mathrm{R}}}{\partial \ln m_{\mathrm{R}}} = \beta_{\mathrm{R}}(\lambda_{\mathrm{R}}), \tag{3.136}$$

$$\ln m_{\mathrm{R}} = \int^{\lambda_{\mathrm{R}}} \frac{dx}{\beta_{\mathrm{R}}(x)}, \tag{3.137}$$

$$= \int^{\lambda_{\mathrm{R}}} dx \left[\frac{1}{\beta_1 x^2} - \frac{\beta_2}{\beta_1^2 x} + O(1) \right], \tag{3.138}$$

$$= -\frac{1}{\beta_1 \lambda_{\mathrm{R}}} - \frac{\beta_2}{\beta_1^2} \ln(\beta_1 \lambda_{\mathrm{R}}) + \ln C_1 + O(\lambda_{\mathrm{R}}). \tag{3.139}$$

https://doi.org/10.1017/9781009402705.004 Published online by Cambridge University Press

Here C_1 is an integration constant, which becomes dependent on the bare λ once the solution is matched to the hopping expansion. (Part of the integration constant is written as $-(\beta_2/\beta_1^2)\ln\beta_1$.) Notice that knowledge of β_2 is needed in order to be able to define $C_1(\lambda)$ as $\lambda_{\rm R} \to 0$. Eq. (3.139) can also be written as

$$m_{\rm R} = C_1(\beta_1\lambda_{\rm R})^{-\beta_2/\beta_1^2} e^{-1/\beta_1\lambda_{\rm R}}[1 + O(\lambda_{\rm R})], \tag{3.140}$$

which shows that $m_{\rm R}$ depends non-analytically on $\lambda_{\rm R}$ for $\lambda_{\rm R} \to 0$. Lüscher and Weisz show that similarly

$$Z = C_2[1 + O(\lambda_{\rm R})], \tag{3.141}$$

$$\kappa_{\rm c} - \kappa = C_3 m_{\rm R}^2(\lambda_{\rm R})^{\delta_1/\beta_1}[1 + O(\lambda_{\rm R})], \tag{3.142}$$

where δ_1 is a Callan–Symanzik coefficient similar to the β's.

From these equations follow the scalings laws, $\tau = 1 - \kappa/\kappa_{\rm c} \to 0$:

$$m_{\rm R} \to C_4\tau^{1/2}|\ln\tau|^{\delta_1/2\beta_1}, \tag{3.143}$$

$$\lambda_{\rm R} \to \frac{2}{\beta_1}|\ln\tau|^{-1}, \tag{3.144}$$

$$Z \to C_2. \tag{3.145}$$

We recognize that the behavior (3.144) follows from (3.100). Note that (3.143) shows that the correlation-length critical exponent ν has almost the mean-field value $\nu = \frac{1}{2}$: it is modified only by a power of $\ln\tau$.

In the scaling limit all information about the renormalized coupling coming from the hopping expansion is contained in $C_1(\lambda)$, which increases monotonically with decreasing λ. For small bare coupling C_1 can be calculated with the weak-coupling expansion. In fact, inserting the expansion (3.86) for $\lambda_{\rm R}$ into (3.140) and expanding in λ_0 leads to

$$\ln C_1(\lambda) = \frac{1}{\beta_1\lambda_0} + \frac{\beta_2}{\beta_1^2}\ln(\beta_1\lambda_0) - \frac{c}{2} + O(\lambda_0). \tag{3.146}$$

For infinite bare coupling Lüscher and Weisz find $C_1(\infty) = \exp(1.5)$. The fact that $C_1(\lambda)$ decreases as λ increases corresponds to the intuition that for given $m_{\rm R}$, the renormalized coupling increases with λ. Conversely, for given $\lambda_{\rm R}$, the smallest lattice spacing (smallest $m_{\rm R}$) is obtained with the largest λ, i.e. $\lambda = \infty$.

The hopping expansion holds in the region of the phase diagram connected to the line $\kappa = 0$, i.e. the symmetric phase. Lüscher and Weisz extended these results into the physically relevant broken phase, where relations similar to (3.140)–(3.145) were obtained with coefficients

C' (the Callan–Symanzik coefficients are the same in both phases). They considered the critical theory at $\kappa = \kappa_c$ and used perturbation theory in $\kappa - \kappa_c$, or equivalently m_R^2, to connect the symmetric and broken phases. This is done again using renormalized perturbation theory with the results

$$C'_1(\lambda) = 1.435\, C_1(\lambda), \quad C'_{2,3}(\lambda) = C_{2,3}(\lambda). \tag{3.147}$$

Another definition was chosen for the renormalized coupling in the broken phase, which is very convenient:

$$\lambda_R = \frac{m_R^2}{2v_R^2}, \quad v_R \equiv Z_\pi^{-1/2} v = Z_\pi^{-1/2} \langle\phi\rangle, \tag{3.148}$$

where Z_π is the wave-function renormalization constant of the Goldstone bosons. This choice is identical in form to the classical relation between the coupling, mass and vacuum expectation value (cf. (3.10)). The renormalized coupling in the broken phase cannot be defined at zero momentum, as in the symmetric phase, because the massless Goldstone bosons would lead to infrared divergences (in absence of explicit symmetry breaking). Using Z_π in the definition of v_R allows the identification of v_R with the pion decay constant f_π in the application of the $O(4)$ model to low-energy pion physics, or with the electroweak scale of 246 GeV in the application to the Standard Model.

The renormalization-group equations were numerically integrated again in the broken phase, this time for increasing m_R, until the renormalized λ_R became too large and the perturbative beta function could no longer be trusted. We mention here the result $\lambda_R < 3.5$ for $m_R < 0.5$, at $\lambda = \infty$. Hence, also in the broken phase the renormalized coupling is relatively small even at the edge of the scaling region, taken somewhat arbitrarily to be at $m_R = 0.5$, and the renormalized coupling goes to zero in the continuum limit $m_R \to 0$.

Figure 3.12 shows lines of constant renormalized coupling with varying κ/κ_c for the case $n = 1$ [21]. For a given λ_R we can go deeper into the scaling region, i.e. approach the critical line $\kappa/\kappa_c = 1$ by increasing the bare coupling λ. This behavior was also found in the weak-coupling expansion, but the results there became invalid as λ grew too big. Here we see that the behavior continues for large λ and that the line $\lambda = \infty$ is reached before reaching the critical line. The critical line can be approached arbitrarily closely only for arbitrarily small renormalized coupling. It follows that the beta function of the model has to correspond to case (b) in figure 3.7.

https://doi.org/10.1017/9781009402705.004 Published online by Cambridge University Press

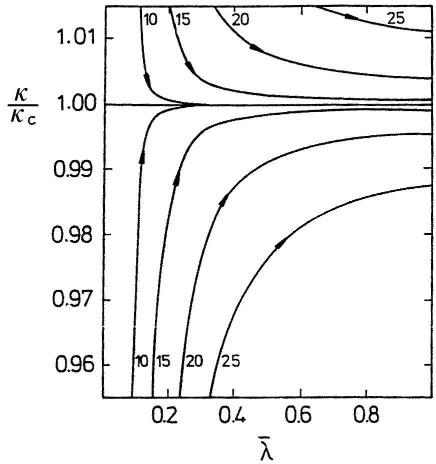

Fig. 3.12. Lines of constant renormalized coupling for the case $n = 1$ determined by Lüscher and Weisz. The lines are labeled by the value of $g_{\mathrm{R}} \equiv 6\lambda_{\mathrm{R}}$. The bare coupling λ increases from 0 to ∞ as the LW parameter $\bar{\lambda}$ goes from 0 to 1. From [21].

For the $O(4)$ model, the figure corresponding to 3.12 is similar, except that the values of λ_{R} at a given am_{R} are smaller [23]. The first beta-function coefficient increases with n, so one expects the renormalization effects to be larger than for $n = 1$.

Let us recall here another well-known criterion for a coupling being small or large: the unitarity bound. This is the value of the renormalized coupling at which the lowest-order approximation to the elastic scattering amplitude T becomes larger than a bound deduced from the unitarity of the scattering matrix S. In a partial wave state of definite angular momentum (e.g. the s-wave) the scattering matrix is finite dimensional, its eigenvalues are phase factors $S = \exp(i2\delta)$, with δ the standard phase shifts. Since the lowest-order (Born) approximation is real and $T = (S-1)/i = 2\exp(i\delta)\sin\delta$ has a real part $\in (-1,1)$, one requires the Born approximation for $|T|$ to be smaller than 1. This gives an upper bound on λ_{R}: the unitarity bound. The maximum values of the renormalized coupling at $m_{\mathrm{R}} = 0.5$ turn out to be smaller than the unitarity bound (in the broken phase the maximum λ_{R} is only about two thirds of this bound).

Summarizing, the results show that the $O(n)$ models (in particular the cases $n = 1$ and 4) in four dimensions are 'trivial': the renormalized coupling vanishes in the continuum limit. Since we want of course an interacting model we cannot take the lattice distance to zero. The model is to be interpreted as an effective model that is valid at momenta much smaller than the cutoff π (π/a in physical units). For not too large renormalized coupling the cutoff can be huge and lattice artifacts very small. At the scale of the cutoff the model loses its validity, and in realistic applications new physical input is needed. Where this happens depends on the circumstances. The relevance of these results for the Standard Model will be discussed later.

3.9 Numerical simulation

With numerical simulations we get non-perturbative results albeit on finite lattices. Simulations provide furthermore a valuable kind of insight into the properties of the systems, which is complementary to expansions in some parameter.

The lattice is usually taken of the form $N^3 \times N_t$, with $N = 4, 6, 8, \ldots$, and N_t of the same order. For simplicity we shall assume that $N_t = N$ in the following. For the $O(4)$ model sizes 10^4–16^4 are already very useful. Expectation values

$$\langle O \rangle = \frac{1}{Z} \int D\phi \, \exp[S(\phi)] \, O(\phi) \tag{3.149}$$

are evaluated by producing a set of field configurations $\{\phi_x^\alpha\}_j$, $j = 1, \ldots, K$, which is distributed according to the weight factor $\exp S(\phi)$, giving the approximate result

$$\langle O \rangle \approx \overline{O} \equiv \frac{1}{K} \sum_{j=1}^{K} O(\phi_j), \tag{3.150}$$

with a statistical error $\propto 1/\sqrt{K}$. The ensemble is generated with a stochastic process, e.g. using a Metropolis or a Langevin algorithm. We shall give only a brief description of the Monte Carlo methods and the analysis of the results. Monte Carlo methods are described in more detail in [4, 6, 10].

For example, a Langevin simulation produces a sequence $\phi_{x,n}^\alpha$, $n = 1, 2, \ldots$, by the rule

$$\phi_{x,n+1}^\alpha = \phi_{x,n}^\alpha + \delta \frac{\partial S(\phi_n)}{\partial \phi_{x,n}^\alpha} + \sqrt{2\delta}\, \eta_{x,n}^\alpha, \tag{3.151}$$

https://doi.org/10.1017/9781009402705.004 Published online by Cambridge University Press

where $\eta_{x,n}^{\alpha}$ are Gaussian pseudo-random numbers with unit variance and zero mean,

$$\langle \eta_{x,n}^{\alpha} \rangle = 0, \quad \langle \eta_{x,n}^{\alpha} \eta_{x',n'}^{\alpha'} \rangle = \delta_{\alpha\alpha'} \delta_{xx'} \delta_{nn'}, \tag{3.152}$$

and δ is a step size related to the Langevin time t by $t = \delta n$. It can be shown that as $t \to \infty$, the ϕ's become distributed according to the desired $\exp S(\phi)$, up to terms of order δ (cf. problem (viii)). Using a small δ such as 0.01, the system reaches equilibrium after some time, in units related to the mass gap of the model, and configurations ϕ_j may be recorded every $\Delta t = 1$, say. The finite δ produces a systematic error, which can be reduced by taking δ sufficiently small, or by using several δ's and extrapolating to $\delta = 0$. The configurations j and $j+1$ are usually correlated, such that the true statistical error is larger than the naive standard deviation

$$\sqrt{\frac{1}{K} \sum_{j=1}^{K} \left(O(\phi_j) - \overline{O}\right)^2} \tag{3.153}$$

but there are methods to take care of this.

The Metropolis algorithm is often preferred over the Langevin one, since it does not suffer from systematic step-size errors $\propto \delta$ and it is often more efficient. Research into efficient algorithms is fascinating and requires good insight into the nature of the system under investigation. New algorithms are being reported every year in the 'Lattice proceedings'.

Since the lattices are finite, we have to take into account systematic errors due to scaling ($O(a)$) violations and finite-size (L) effects ($L = Na$). It is important to determine these systematic errors and check that they accord with theoretical scaling and finite-size formulas. We can then attempt to extrapolate to infinite volume and zero lattice spacing.

Typical observables O for the $O(n)$ models are the average 'magnetization' $\bar{\phi}^{\alpha} = \sum_x \phi_x^{\alpha}/N^4$, the average 'energy' $-S/N^4$, which reduces to the average 'link' $\sum_{x\mu} \phi_x^{\alpha} \phi_{x+\hat{\mu}}^{\alpha}/4N^4$ in the limit $\lambda \to \infty$, and products like $\phi_x^{\alpha} \phi_y^{\beta}$ giving correlation functions upon averaging. The free energy $F = -\ln Z$ itself cannot be obtained directly by Monte Carlo methods, but may be reconstructed, e.g. by integrating $\partial F/\partial \kappa = -2\langle \sum_{x\mu} \phi_x^{\alpha} \phi_{x+\hat{\mu}}^{\alpha} \rangle$.

The correlation function $G_{xy}^{\alpha\beta} = \langle \phi_x^{\alpha} \phi_y^{\beta} \rangle - \langle \phi_x^{\alpha} \rangle \langle \phi_y^{\beta} \rangle$ is used to determine the masses of particles. With periodic boundary conditions it depends only on the difference $x - y$. For example, in the symmetric

https://doi.org/10.1017/9781009402705.004 Published online by Cambridge University Press

phase the spectral representation can be written as

$$\sum_{\mathbf{x}} e^{-i\mathbf{p}\mathbf{x}} G^{\alpha\alpha}_{\mathbf{x},t;\mathbf{0},0} = \sum_{\gamma} |\langle 0|\phi^{\alpha}|\mathbf{p},\gamma\rangle|^2 \left[e^{-\omega_{\mathbf{p},\gamma}t} + e^{-\omega_{\mathbf{p},\gamma}(N_t-t)}\right], \quad (3.154)$$

where finite-temperature (finite N_t) corrections of the form $\propto$ $\langle\mathbf{p}'\gamma'|\phi^{\alpha}_x|\mathbf{p}\gamma\rangle$ have been neglected. Choosing zero momentum $\mathbf{p}$, one may fit the propagator data for large t and $N_t - t$ to

$$R\cosh\left[m\left(t - \frac{N_t}{2}\right)\right], \quad R = |\langle 0|\phi^{\alpha}|\mathbf{0}\alpha\rangle|^2 \exp\left(-m\frac{N_t}{2}\right), \quad (3.155)$$

where $m = \omega_{\min}$ is the mass of the particle with the quantum numbers of ϕ^{α}. It is assumed that the contributions of the next energy levels ω' with the same quantum numbers (such as three particle intermediate states), which have relative size $\exp[-(\omega' - m)t]$, can be neglected for sufficiently large times. Alternatively, one can try to determine the renormalized mass and wave-function renormalization constant in momentum space from eq. (3.81), but this does not give the particle mass directly. Only when the particle is weakly coupled is $m_{\rm R} \approx m$. The higher-order correlation functions (such as the four-point functions) require in general much better statistics than do the propagators.

For illustration we show first some early results in the symmetric phase. Figure 3.13 shows the particle mass and the renormalized coupling $g_{\rm R} = 6\lambda_{\rm R}$ as functions of the spatial size N in a simulation at infinite bare coupling [24]. We see that the interactions cause the finite-volume mass to increase over the infinite-volume value (the linear extent in physical units, Lm, changes by roughly a factor of two). The results for the coupling constant roughly agree within the errors with those obtained by Lüscher and Weisz using the hopping expansion. Figure 3.14 shows a result [25] for the dressed propagator (correlation function) analyzed in momentum space. The fact that the propagator resembles so closely a free propagator, apart from renormalization, is an indication that the effective interactions are not very strong, despite the large bare coupling.

The broken phase is physically more interesting. Although there is rigorously no phase transition in a finite volume, the difference between the symmetric- and broken-phase regions in parameter space is clear in the simulations. The phase boundary is somewhat smeared out by finite-volume effects. In the broken phase of the $O(n)$ model for $n > 1$, there is a preferred direction, along $\langle\phi^{\alpha}\rangle = v^{\alpha} \neq 0$, and one considers the longitudinal and transverse modes $G_{\sigma} = v^{-2}v^{\alpha}v^{\beta}G^{\alpha\beta}$ and $G_{\pi} = (\delta_{\alpha\beta} - v^{-2}v^{\alpha}v^{\beta})G^{\alpha\beta}/(n-1)$. The latter correspond to the Gold-

https://doi.org/10.1017/9781009402705.004 Published online by Cambridge University Press

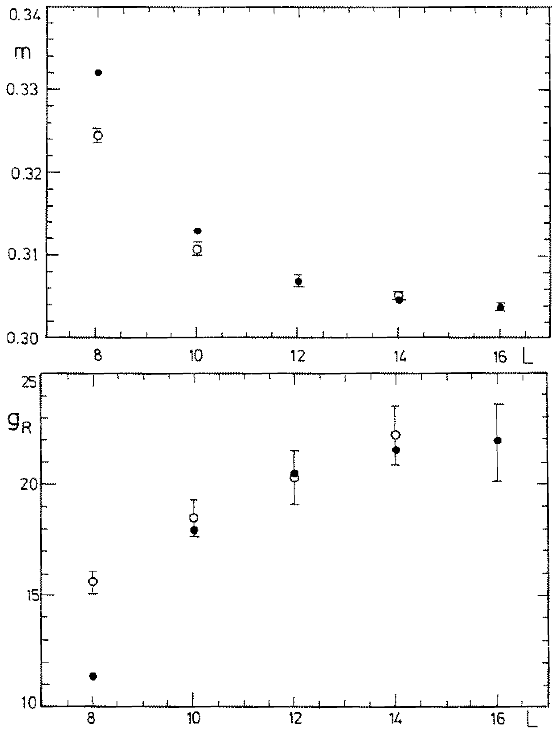

Fig. 3.13. Finite-size dependence of m and $g_{\rm R} = 6\lambda_{\rm R}$ in a simulation in the symmetric phase ($L = N$, $\lambda = \infty$). The full circles correspond to a finite-size dependence expected from renormalized perturbation theory. From [24].

stone bosons. The σ particle can decay into the π particles, which leads to complications in the analysis of the numerical data. The Goldstone bosons lead to strong finite-size effects. Finite-size effects depend on the range of the interactions, the correlation length, which is infinite for the Goldstone bosons. However, the finite size also gives a non-zero mass to the Goldstone bosons. These effects have to be taken into account in the analysis of the simulation results. The theoretical analysis is based on effective actions, using 'chiral perturbation theory' or 'renormalized perturbation theory'.

Consider the magnetization observable $\bar{\phi}^\alpha = \sum_x \phi_x^\alpha / N^4$. An impression of its typical distribution is illustrated in figure 3.15. The difference between the symmetric and broken phase is clear, yet the figure suggests correctly that the angular average leads to $\langle \bar{\phi}^\alpha \rangle = 0$ also in the broken-phase region. In a finite volume there is no spontaneous

https://doi.org/10.1017/9781009402705.004 Published online by Cambridge University Press

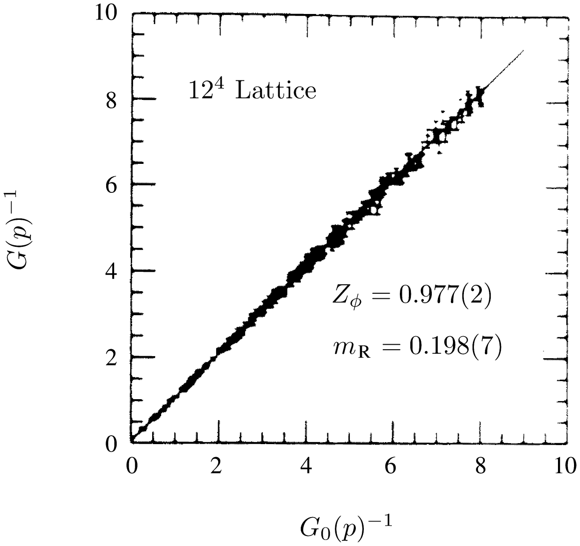

Fig. 3.14. Dressed propagator in momentum space plotted as a function of $\sum_\mu 4\sin^2(p_\mu/2)$, at $m_0^2 = -24.6$, $\lambda_0 = 100$. From [25].

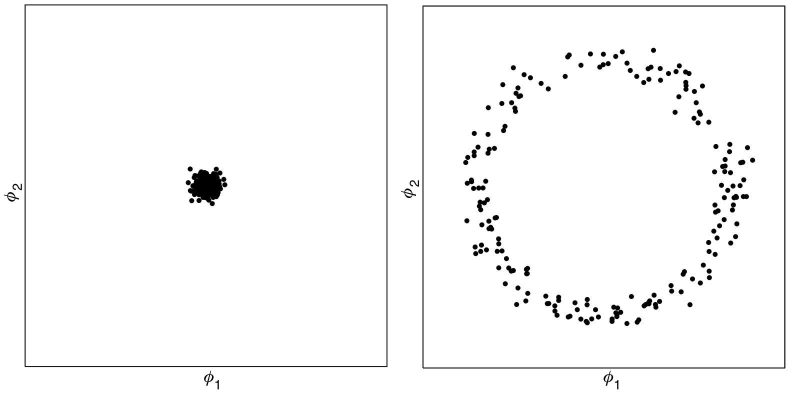

Fig. 3.15. Qualitative illustration of the probability distribution of $\bar{\phi}^\alpha$ at finite volume for $n = 2$ in the symmetric phase (left) and the broken phase (right).

symmetry breaking. To formulate a precise definition of v^α, we introduce an explicit symmetry-breaking term into the action, which 'pulls' the spins along a direction, say 0,

$$\Delta S = \epsilon \sum_x \phi_x^0, \tag{3.156}$$

and define

$$v^\alpha = \lim_{\epsilon\to 0} \lim_{L\to\infty} \langle \phi_x^\alpha \rangle, \tag{3.157}$$

where the order of the limits is crucial. To understand this somewhat better, one introduces the constrained effective potential $V_{\rm L}(\bar\phi)$, which is obtained by integrating over all field configurations with the constraint $\bar\phi^\alpha = \sum_x \phi_x^\alpha / L^4$,

$$\exp(-L^4 V_{\rm L}(\bar\phi)) = \int D\phi\, \exp[S(\phi)]\, \delta\left(\bar\phi^\alpha - \sum_x \phi_x^\alpha / L^4\right), \tag{3.158}$$

such that

$$Z = \int d^n\bar\phi\, \exp\bigl[-L^4 V_{\rm L}(\bar\phi)\bigr], \tag{3.159}$$

and

$$\langle \bar\phi^\alpha \rangle = \frac{\int d^n\bar\phi\, \exp\bigl[-L^4 V_{\rm L}(\bar\phi)\bigr]\, \bar\phi^\alpha}{\int d^n\bar\phi\, \exp\bigl[-L^4 V_{\rm L}(\bar\phi)\bigr]}. \tag{3.160}$$

The fact that the effective potential comes with a factor L^4 is easily understood from the lowest-order approximation in $\lambda \to 0$, which is obtained by simply inserting the constant $\bar\phi^\alpha$ for ϕ_x^α in the classical action,

$$S(\bar\phi) = -L^4 V_{\rm L}(\bar\phi) = -N^4[(1-8\kappa)\bar\phi^2 + \lambda(\bar\phi^2 - 1)^2 - \epsilon\bar\phi^0], \tag{3.161}$$

where we used the form (3.16) of the action in lattice units. In this classical approximation the constraint effective potential is independent of L. The exact constraint effective potential is only weakly dependent on L, for sufficiently large L, and as L increases the integrals in (3.160) are accurately given by the saddle-point approximation, i.e. by the sum over the minima of $V_{\rm L}(\bar\phi)$. In absence of the ϵ term there is a continuum of saddle points and $\langle \bar\phi^\alpha \rangle = 0$ even in the broken phase. A unique saddle point is obtained, however, for non-zero ϵ. If we let ϵ go to zero after the infinite-volume limit, $\langle \bar\phi^\alpha \rangle$ remains non-zero. For more information on the constraint effective potential, see e.g. [26].

This technique of introducing explicit symmetry breaking is used in simulations [27] as shown in figure 3.16. A simpler estimate of the infinite-volume value v of the magnetization is obtained with the 'rotation method', in which the magnetization of each individual configuration is rotated to a standard direction before averaging. The resulting $\langle |\bar\phi| \rangle$ can be fitted to a form $v + \text{constant} \times N^{-2}$.

https://doi.org/10.1017/9781009402705.004 Published online by Cambridge University Press

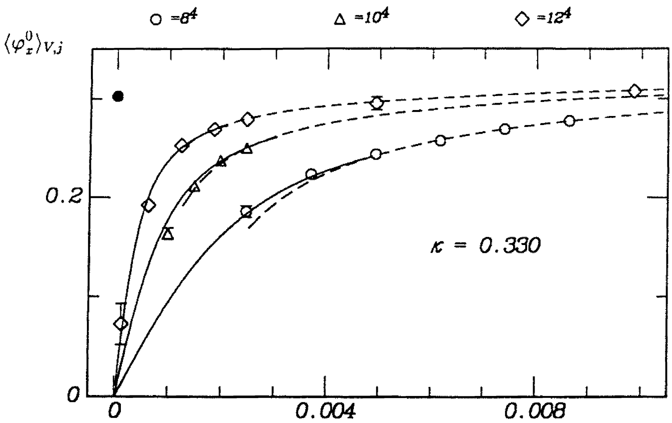

Fig. 3.16. Plots of $\langle\bar{\phi}^4\rangle$ as a function of $j = \epsilon$ in the $O(4)$ model for various lattice sizes. The data are fitted to the theoretical behavior (curves) and extrapolated to infinite-volume and $\epsilon = 0$, giving the full circle in the upper left-hand corner. From [27].

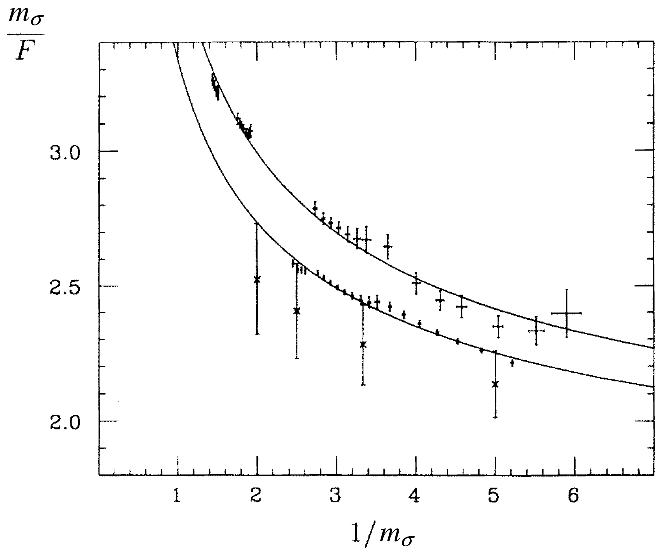

Fig. 3.17. Results on $m_\sigma/F = m_\sigma/v_R$ as a function of the correlation length $1/m_\sigma$, for the 'standard (usual) action' (lower data) and a 'Symanzik-improved action' (upper data). The crosses are results of Lüscher and Weisz obtained with the hopping expansion. The bare coupling $\lambda = \infty$. The curves are interpolations based on renormalized perturbation theory. From [28].

As a last example we show in figure 3.17 results on the renormalized coupling $\sqrt{2\lambda_{\rm R}} = m_{\rm R}/v_{\rm R}$ [28]. Data are shown for the action considered here (the 'standard action') and for a 'Symanzik-improved action'. We see that the data for the standard action agree with the results obtained with the hopping expansion in the previous section, within errors. The Symanzik-improved action has next-to-nearest-neighbor couplings such that the $O(a^2)$ errors are eliminated in the classical continuum limit. It is not clear *a priori* that this leads to better scaling in the quantum theory, because the scalar field configurations that contribute to the path integral are not smooth on the lattice scale, but it is interesting that the different regularization leads to somewhat larger renormalized couplings for a given correlation length.

In conclusion, the numerical simulations have led to accurate results which fully support the theoretical understanding that the $O(n)$ models are 'trivial'.

3.10 Real-space renormalization group and universality

One of the cornerstones of quantum field theory is universality: the physical properties emerging in the scaling region are to a large extent independent of the details of formulating the theory on the scale of the cutoff. The physics of the $O(n)$ models is expected to be independent of the lattice shape, the addition of next-nearest-neighbor couplings, next-next-nearest-neighbor couplings, ..., or higher-order terms $(\phi^2)^k$, $k = 3, 4, \ldots$ (of course, in its Ising limit or non-linear sigma limit where $\phi^2 = 1$ such higher-order terms no longer play a role). More precisely, the physical outcome of the models falls into universality classes, depending on the symmetries of the system and the dimensionality of space–time. Our understanding of universality comes from the renormalization group *à la* Wilson [29, 30] ('block spinning', see e.g. [11]), and from the weak-coupling expansion. We shall sketch the ideas using the one-component scalar field as an example, starting with the block spinning approach used in the theory of critical phenomena.

In the real-space renormalization-group method one imagines integrating out the degrees of freedom with wave lengths of order of the lattice distance and expressing the result in terms of an effective action for the remaining variables. On iterating this procedure one obtains the effective action describing the theory at physical ($\gg a$) distance scales.

Let $\bar{\phi}_{\bar{x}}$ be the average of ϕ_x over a region of linear size s around $\bar{x}$,

$$\bar{\phi}_{\bar{x}} = \sum_x B_{\bar{x},x}\phi_x. \tag{3.162}$$

The averaging function $B(\bar{x}, x)$ is concentrated near sites $\bar{x}$ on a coarser lattice that are a distance s apart in units of the original lattice. We could simply take values $\bar{x}_\mu = 2x_\mu$ with $B_{x,\bar{x}} = z\sum_\mu \delta_{\bar{x}\pm\hat{\mu},x}$ ('blocking'), or a smoother Gaussian average $B = z\sum_x \exp(-(x-\bar{x})^2/2s)$, with suitable normalization factors z. The effective action $\bar{S}$ is defined by

$$e^{\bar{S}(\bar{\phi})} = \int D\phi\, e^{S(\phi)} \prod_{\bar{x}} \delta\left(\bar{\phi}_{\bar{x}} - \sum_x B_{\bar{x},x}\phi_x\right), \tag{3.163}$$

and it satisfies

$$\int D\bar{\phi}\, e^{\bar{S}(\bar{\phi})} = \int D\phi\, e^{S(\phi)}. \tag{3.164}$$

After a few iterations the effective action has many types of terms, so one is led to consider general actions of the form

$$S(\phi) = \sum_\alpha K_\alpha O_\alpha(\phi). \tag{3.165}$$

Here O_α denotes terms of the schematic form $(\partial_\mu\phi\partial_\mu\phi)^k$, $(\phi^2)^k$, $\ldots$ $(k = 1, 2, \ldots)$. The new effective action can then again be written in the form

$$\bar{S}(\bar{\phi}) = \sum_\alpha \bar{K}_\alpha O_\alpha(\bar{\phi}). \tag{3.166}$$

The scale factor z in the definition of the averaging function B is chosen such that the coefficient of $\partial_\mu\bar{\phi}\partial_\mu\bar{\phi}$ is equal to $\frac{1}{2}$, in lattice units of the coarse $\bar{x}$ lattice, in order that the new coefficients $\bar{K}_\alpha$ do not run away after many iterations. Because of the locality of the averaging function one expects the action $\bar{S}$ to be local too, i.e. the range of the couplings in $\bar{S}$ is effectively finite, and one expects the dependence of the coefficients $\bar{K}_\alpha$ on K_α to be analytic. One iteration thus constitutes a renormalization-group transformation

$$\bar{K}_\alpha = T_\alpha(K). \tag{3.167}$$

We can still calculate correlation functions and quantities of physical interest with the new fields $\bar{\phi}$. For these the highest-momentum contributions are suppressed by the averaging, as can be seen by expressing them in terms of the original fields ϕ, but contributions from physical momenta which are low compared to the cutoff are unaffected. In particular the correlation length in units of the original lattice distance is unchanged. However, in units of the $\bar{x}$ lattice distance the correlation length is smaller by a factor $1/s$. Each iteration the correlation length is shortened by a factor $1/s$ and when it is of order one we imagine stopping the iterations. We can then still extract the physics on the momentum scales of order of the mass scale. If we want to discuss scales ten times higher, we can stop iterating when the correlation length is still of order ten.

In the infinite dimensional space of coupling constants K_α there is a hypersurface where the correlation length is infinite, the critical surface. We want to start our iterations very close to the critical surface because we want a large correlation length on the original lattice, which means that we are able to do many iterations before the correlation length is of order unity. If there is a fixed point K^*,

$$T_\alpha(K^*) = K^*_\alpha, \tag{3.168}$$

then we can perform many iterations near such a point without changing the K_α very much. At such a fixed point the correlation length does not change, so it is either zero or infinite. We are of course particularly interested in fixed points in the critical surface. Linearizing about such a critical fixed point (on the critical surface),

$$\bar{K}_\alpha - K^*_\alpha = M_{\alpha\beta}(K_\beta - K^*_\beta), \quad M_{\alpha\beta} = [\partial T_\alpha/\partial K_\beta]_{K=K^*}\,, \tag{3.169}$$

it follows that the eigenvalues λ_i of $M_{\alpha\beta}$ determine the attractive ($\lambda_i < 1$) or repulsive ($\lambda_i > 1$) directions of the 'flow'. These directions are given by the corresponding eigenvectors e_i^α, which determine the combinations $e_i^\alpha O_\alpha$.

One expects only a few repulsive eigenvalues, called 'relevant', while most of them are attractive and called 'irrelevant'. Eigenvalues $\lambda_i = 1$ are called marginal. Further away from the fixed point the attractive and repulsive directions will smoothly deform into attractive and repulsive curves. The marginal directions will also turn into either attractive or repulsive curves.

Let us start the iteration somewhere on the critical surface. Then the flow stays on the surface. Suppose that the flow on the surface is attracted to a critical fixed point K^*. Next let us start very close to the critical surface. Then the flow will at first still be attracted to K^*, but, since with each iteration the correlation length decreases by a factor $1/s$, the flow moves away from the critical surface and eventually turns away from the fixed point. Hence the critical fixed point has at least one relevant direction away from the critical surface.

https://doi.org/10.1017/9781009402705.004 Published online by Cambridge University Press

Suppose there is only one such relevant direction (and its opposite on the other side of the critical surface). Then, after many iterations the flow just follows the flow-line through this relevant direction. The physics is then completely determined by the flow-line through the relevant direction: the physical trajectory (also called the renormalized trajectory). To the relevant direction there corresponds the only free parameter we end up with: the ratio cutoff/mass, Λ/m (where $\Lambda = \pi/a$). This ratio is determined by the initial distance to the critical surface, or equivalently, by the number of iterations and the final distance to the critical surface where we stop the iterations. However, the mass just sets the dimensional scale of the theory and there is no physical free parameter at all under these circumstances. All the physical properties (e.g. the renormalized vertex functions and the renormalized coupling $\lambda_{\rm R}$) are fixed by the properties of the physical trajectory. On the other hand, each additional relevant direction offers the possibility of an additional free physical parameter, which may be tuned by choosing appropriate initial conditions.

Many years of investigation have led to the picture that there is only one type of critical fixed point in the $O(n)$ symmetric models, which has only one relevant direction corresponding to the mass as described above, and one marginal but attractive direction corresponding to the renormalized coupling. This means that eventually the renormalized coupling will vanish after an infinite number of iterations (triviality). This is the reason that the fixed point is called 'Gaussian', for the corresponding effective action is quadratic. However, because the renormalized coupling is marginal and therefore changes very slowly near the critical point, it can still be substantially different from zero even after very many iterations (very large Λ/m ratios). With a given number of iterations we can imagine maximizing the renormalized coupling over all possible initial actions parameterized by K_α, giving an upper bound on the renormalized coupling. Within its upper bound the renormalized coupling is then still a free parameter in the models. The situation is illustrated in figure 3.18.

For the massless theory the correlation length is infinite, so we start on the critical surface. The flow is attracted to K^*, which determines the physics outcome. The marginally attractive direction corresponds in the massless case to the running renormalized coupling $\bar{\lambda}(\mu)$ at some physical momentum scale μ. Each iteration the maximum momentum scale is lowered by a factor $1/s$ and, after many iterations, the ratio (maximum momentum scale)/cutoff is very small. We stop the iteration

https://doi.org/10.1017/9781009402705.004 Published online by Cambridge University Press

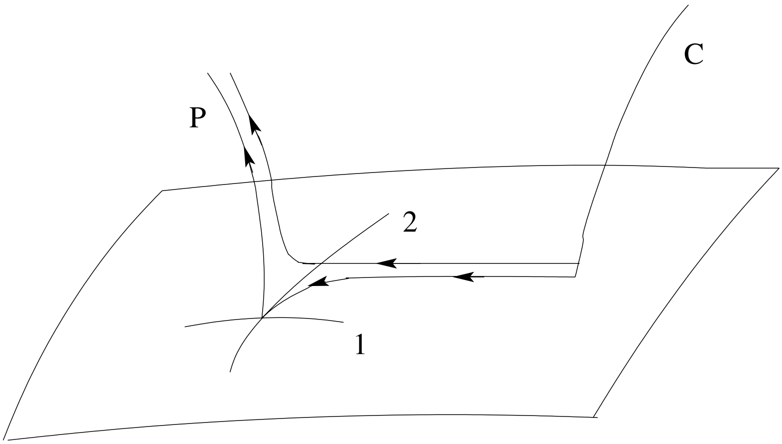

Fig. 3.18. Renormalization group-flow in ϕ^4 theory. The line C represents the 'canonical surface' of actions of the standard form $S = 2\kappa \sum_{x\mu} \phi_x \phi_{x+\hat{\mu}} - \sum_x [\phi_x^2 + \lambda(\phi_x^2 - 1)^2]$. The line P represents the physical trajectory. Direction 1 is an irrelevant direction, direction 2 represents the marginal direction corresponding to the renormalized coupling. Shown are two flows starting from a point in C, one near the critical surface and on this surface.

when the maximum momentum scale is of order μ. For a given number of iterations the running coupling can still vary within its upper bound. As the number of iterations goes to infinity, μ has to go to zero and $\bar{\lambda}(\mu) \to 0$ because the flow along the marginal direction is attracted to zero coupling. So the massless theory can be defined by taking the number of iterations ($\propto \Lambda/\mu$) large but finite, and $\bar{\lambda}(\mu) \to 0$ as $\mu \to 0$.

The critical fixed points of the real-space renormalization-group transformation give a very attractive explanation of universality.

3.11 Universality at weak coupling

To formulate a general action at weak coupling we start with the form (3.16) and first make a scale transformation $\phi = \phi'/\sqrt{\lambda}$, which brings the action into the form

$$S(\phi') = \frac{1}{\lambda} \sum_x \left[2\kappa \sum_\mu \phi'_x \phi'_{x+\hat{\mu}} - \phi_x^{'2} - (\phi_x^{'2} - 1)^2 \right]. \qquad (3.170)$$

We see that λ appears as a natural expansion parameter for a saddle-point expansion, while the other coefficients in the action are of order

https://doi.org/10.1017/9781009402705.004 Published online by Cambridge University Press

one in lattice units. A natural generalization is given by

$$S(\phi') = \frac{1}{\lambda} \sum_x \left[2\kappa \sum_\mu \phi'_x \phi'_{x+\hat\mu} + \kappa' \sum_{\mu<\nu} \phi'_x \phi'_{x+\hat\mu+\hat\nu} \right. \tag{3.171}$$

$$\left. + \kappa'' \sum_\mu \phi'_x \phi'_{x+2\hat\mu} + \kappa''' \sum_\mu \phi'^2_x \phi'^2_{x+\hat\mu} + \cdots - \sum_{k=1}^{\infty} v_{2k} \phi'^{2k}_x \right],$$

which still has the symmetry $\phi \to -\phi$. The coefficients in this expression are supposed to be of order 1.

The parameter λ enters in the same place as Planck's constant $\hbar$ when we introduced the path-integral quantization method, before we set it equal to 1. It can be shown that the expansion in powers of $\hbar$ corresponds to an expansion in the number of loops in Feynman diagrams. For this reason the weak-coupling expansion is called the semiclassical expansion.

For convenience in the following we shall use the original continuum-motivated parameterization (3.13) with the field $\varphi = \phi/\sqrt{2\kappa}$ and rewrite (3.171) in the form

$$\begin{aligned} S &= -\frac{1}{\lambda_0} \sum_x \left[\frac{1}{2} \partial_\mu \varphi'_x \partial_\mu \varphi'_x + z \partial_\mu \varphi'^2_x \partial_\mu \varphi'^2_x + \cdots + \sum_k u_{2k}\, \varphi'^{2k}_x \right] \\ &= -\sum_x \left[\frac{1}{2} \partial_\mu \varphi_x \partial_\mu \varphi_x + \lambda_0 z \partial_\mu \varphi^2_x \partial_\mu \varphi^2_x + \cdots + \sum_k \lambda_0^{k-1} u_{2k} \varphi^{2k}_x \right], \end{aligned} \tag{3.172}$$

where $\varphi' = \sqrt{\lambda_0}\varphi$. Here again the coefficients $z, \ldots,$ and u_{2k} are supposed to be dimensionless numbers of order unity, with the exception of u_2 which becomes $m^2_{0\mathrm{c}} = O(\lambda_0)$ at the phase boundary (this is special to the continuum parameterization). It is instructive to rewrite the generic action (3.172) in physical units,

$$S = -\sum_x \left(\frac{1}{2} \partial_\mu \varphi_x \partial_\mu \varphi_x + a^2 \lambda_0 z \partial_\mu \varphi^2_x \partial_\mu \varphi^2_x + \cdots \right.$$

$$\left. + \sum_k a^{2k-4} \lambda_0^{k-1} u_{2k} \varphi^{2k}_x \right), \tag{3.173}$$

where now $\partial_\mu \varphi_x = (\varphi_{x+a_\mu} - \varphi_x)/a$ and $\sum_x$ contains a factor a^4. The higher-dimensional operators are accompanied by powers of the lattice distance a such that the action is dimensionless.

In the classical continuum limit $a \to 0$ we end up with just the φ^4 theory, with u_2 chosen such that $m^2 = 2u_2 a^{-2}$ remains finite. In other

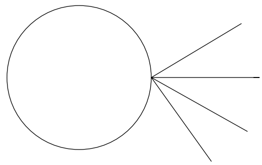

Fig. 3.19. Contribution of the bare six-point vertex to $\Gamma_{(4)}$.

words, the bare two- and four-point vertex functions take their usual continuum limits and the higher-order bare vertex functions vanish. In non-trivial orders of the semiclassical expansion, the powers of a in the bare vertex functions can be compensated by the divergences in the loop diagrams. For example, consider the effect of the term $-\sum_x \lambda_0^2 u_6 a^2 \varphi_x^6$ on the four-point vertex at one-loop order as given by the diagram in figure 3.19. The bare vertex function in momentum space is $-6!\,\lambda_0^2 u_6 a^2$ and the contribution to $\Gamma_{(4)}$ is given by

$$-\tfrac{1}{2}6!\,\lambda_0^2 u_6 a^2 \int_{-\pi/a}^{\pi/a} \frac{d^4 l}{(2\pi)^4} \frac{1}{m_0^2 + a^{-2}\sum_\mu (2 - 2\cos a l_\mu)} = -\tfrac{1}{2}6!\lambda_0^2 u_6 C_0, \tag{3.174}$$

in the limit $a \to 0$ (the constant C_0 was defined in (3.67)).

By looking at more examples one may convince oneself that the higher-order bare vertex functions just lead to new expressions for the vertex functions in terms of the coefficients in the action, which have, however, the same momentum dependence as before. All lattice artifacts end up in constants like C_0, and in the relation between $\lambda_{\rm R}$ and $m_{\rm R}^2$ to λ_0 and m_0^2, such that the renormalized vertex functions, once expressed in terms of the renormalized coupling $\lambda_{\rm R}$ and renormalized mass parameter $m_{\rm R}$, are universal, order by order in perturbation theory.

There is one aspect worth mentioning: the effect of the lattice symmetries. Consider the two-point vertex function in one-loop order, which has the form $\Gamma_{(2)}(p) = a^{-2} f(ap, am_0)$ on dimensional grounds. For $a \to 0$ this takes the form $a^{-2}(\tau a^2 m_0^2 + \tau_{\mu\nu} a^2 p_\mu p_\nu)$ + logarithms. We have seen in section 3.4 how the logarithms emerge from the integration over the loop variable near the origin in momentum space where the lattice expressions take their classical continuum form: the terms containing logarithms are covariant under continuous rotations. What about the polynomial $\tau_{\mu\nu} p_\mu p_\nu$? Its coefficient $\tau_{\mu\nu}$ depends on lattice details, the loop integrations over the cosines near the edge of the Brillouin zone in momentum space. Here the lattice symmetries come to help. The

https://doi.org/10.1017/9781009402705.004 Published online by Cambridge University Press

polynomial has to be invariant under the cubic rotations

$$R^{(\rho\sigma)}:\ x_\rho \to x_\sigma,\ x_\sigma \to -x_\rho,\ x_{\mu\neq\rho,\sigma} \to x_\mu \tag{3.175}$$

and axis reversals

$$I^{(\rho)}:\ x_\rho \to -x_\rho,\ x_{\mu\neq\rho} \to x_\mu. \tag{3.176}$$

There is only one such polynomial: $p^2 = p_1^2 + \cdots + p_4^2$. So the lattice symmetries and dimensional effects are important in order to get covariant renormalized vertex functions. Dimensional analysis showed that the above polynomial is at most of second order and even in $p_\mu \to -p_\mu$ because of axis-reversal symmetry. Note that there is more than one fourth-order polynomial $\tau_{\kappa\lambda\mu\nu}p_\kappa p_\lambda p_\mu p_\nu$ that is invariant under the lattice symmetries. Such polynomials go together with dimensional couplings, such as cutoff effects $\propto a^2$. The polynomials are called *contact terms*, because they correspond in position space to Dirac delta functions and derivatives thereof.

If we destroy the space–time symmetry of the lattice, e.g. by having different couplings in the space and time directions, then we may have to *tune* the couplings in the action to regain covariance in the scaling region.

3.12 Triviality and the Standard Model

Arguments that scalar field models are trivial in the sense that they become non-interacting when the regularization is removed were first given by Wilson, using his formulation of the renormalization group [29, 30]. The arguments imply that triviality should hold within a universality class of bare actions, e.g. next-to-nearest-neighbor couplings, ... In the previous sections we reviewed some calculations and numerical simulations leading to accurate determination of the renormalized coupling in the $O(4)$ model in the broken phase. The $O(4)$ model may be identified with the scalar Higgs sector of the Standard Model, and we shall now review the implications and applications of triviality.

First we review how the $O(4)$ model is embedded in the Standard Model. The action for the Higgs field is given by

$$S_{\rm H} = -\int d^4x\,[(D_\mu\varphi)^\dagger D_\mu\varphi + m_0^2\varphi^\dagger\varphi + \lambda_0(\varphi^\dagger\varphi)^2], \tag{3.177}$$

$$D_\mu\varphi = \left(\partial_\mu - ig_1\frac{1}{2}B_\mu - ig_2 W_\mu^k\frac{\tau_k}{2}\right)\varphi, \tag{3.178}$$

https://doi.org/10.1017/9781009402705.004 Published online by Cambridge University Press

where τ_k are the Pauli matrices, $\varphi = (\varphi_u, \varphi_d)^{\mathrm{T}}$ is the complex Higgs doublet and B_μ, and W_μ^k are the $U(1) \times SU(2)$ electroweak gauge fields. Setting the gauge couplings to zero, the action becomes equivalent to the $O(4)$ model,

$$S_{|g=0} = -\int d^4x \, [\partial_\mu\varphi^\dagger\partial_\mu\varphi + m_0^2\varphi^\dagger\varphi + \lambda_0(\varphi^\dagger\varphi)^2] \tag{3.179}$$

$$= -\int d^4x \left[\frac{1}{2}\partial_\mu\varphi^\alpha\partial_\mu\varphi^\alpha + \frac{m_0^2}{2}\varphi^\alpha\varphi^\alpha + \frac{\lambda_0}{4}(\varphi^\alpha\varphi^\alpha)^2\right],$$

$$\varphi_u = \frac{1}{\sqrt{2}}(\varphi^2 + i\varphi^1), \quad \varphi_d = \frac{1}{\sqrt{2}}(\varphi^0 - i\varphi^3). \tag{3.180}$$

The Higgs field enters also in Yukawa couplings with the fermions. In terms of a matrix field ϕ defined by

$$\phi \equiv \sqrt{2}\begin{pmatrix} \varphi_d^* & \varphi_u \\ -\varphi_u^* & \varphi_d \end{pmatrix}, \tag{3.181}$$

$$= \varphi^0 + i\varphi^k\tau_k = \rho V, \quad V \in SU(2), \quad \rho > 0, \tag{3.182}$$

the Yukawa couplings to the quarks can be expressed as

$$S_Y = -\int d^4x \, \bar{\psi}_{cg}(P_{\mathrm{R}}\phi y_g + y_g P_{\mathrm{L}}\phi^\dagger)\psi_{cg}. \tag{3.183}$$

Here $P_{\mathrm{L,R}} = (1 \mp \gamma_5)/2$ are the projectors on the left- and right-handed fermion fields and the summation is over the QCD colors c and generations g. The Yukawa couplings y are diagonal in $SU(2)$ doublet space, $y = y_u(1+\tau_3)/2 + y_d(1-\tau_3)/2$. The Yukawa couplings to the leptons are similar (in the massless neutrino limit the right-handed neutrino fields decouple).

If we insert the vacuum expectation value of the scalar field

$$\varphi = \frac{1}{\sqrt{2}}\begin{pmatrix} 0 \\ v \end{pmatrix}, \tag{3.184}$$

$$\phi = v\mathbb{1}, \tag{3.185}$$

in the action, we find the masses of the vector bosons W and Z and the photon A, from the terms quadratic in the gauge fields, and the masses of the fermions from the Yukawa couplings. Choosing renormalization conditions such that the 'tree-graph' relations remain valid after renormalization, we have

$$m_W^2 = \tfrac{1}{4}g_{2\mathrm{R}}^2\, v_{\mathrm{R}}^2, \quad m_Z^2 = \tfrac{1}{4}(g_{1\mathrm{R}}^2 + g_{2\mathrm{R}}^2)\, v_{\mathrm{R}}^2, \quad m_A = 0, \tag{3.186}$$

$$m_f = y_{\mathrm{R}f}\, v_{\mathrm{R}}, \quad m_{\mathrm{H}}^2 = 2\lambda_{\mathrm{R}}\, v_{\mathrm{R}}^2, \tag{3.187}$$

https://doi.org/10.1017/9781009402705.004 Published online by Cambridge University Press

where f denotes the fermion. From experiment we know

$$v_{\rm R} = 246 \text{ GeV}, \quad g_{1\rm R} = 0.34, \quad g_{2\rm R} = 0.64. \tag{3.188}$$

The electroweak gauge couplings are effectively quite small (recall the typical factors of g^2/π^2 that occur in perturbative expansions). The Yukawa couplings are generally much smaller, as follows from (3.187) and the fact that the fermion masses are generally small ($<$ 5 GeV) on the electroweak scale. Even the much heavier top quark, which has a mass of about 175 GeV has a Yukawa coupling $y_t \approx 0.71$, which is not very large either. The (running) QCD gauge coupling of the strong interactions is also relatively small on the electroweak scale of 100 GeV: $g_{3\rm R} \approx 1.2$.

To discuss the implications of triviality of the $O(4)$ model, let us assume for the moment that all the gauge and Yukawa couplings can be treated as perturbations on scales $v_{\rm R}$ or higher. Furthermore, assume that the Higgs mass is non-zero (we shall comment on these assumptions below). It then follows from the triviality of the $O(4)$ model that the Standard Model itself must be 'trivial'. Because a non-zero Higgs mass implies $\lambda_{\rm R} \neq 0$, the triviality leads to the conclusion that the regularization cannot be removed completely. Consequently the model must lose its validity on the regularization scale. New physical input is required on this momentum or equivalent distance scale.

It would obviously be very interesting if we could predict at which scale new physics has to come into play. To some extent this can be done as follows. If the Higgs mass is not too large such that $\lambda_{\rm R} = m_{\rm H}^2/2v_{\rm R}$ is in the perturbative domain, we can use eq. (3.140) to calculate the cutoff $\Lambda = \pi/a$ in the lattice regularization,

$$\Lambda = m_{\rm H} C(\beta_1\lambda_{\rm R})^{\beta_2/\beta_1^2} \exp(1/\beta_1\lambda_{\rm R})[1 + O(\lambda_{\rm R})], \tag{3.189}$$

where $C = \pi/C_1'(\lambda_0)$. The constant C_1 is minimal, hence Λ maximal, for infinite bare coupling λ_0. We shall assume this in the following, with $C_1'(\infty) = 6.4$ (the value obtained by Lüscher and Weisz). As an example, $m_{\rm H} = 100$ GeV gives $\lambda_{\rm R} = 0.083$ and $\Lambda = 7 \times 10^{36}$ GeV. This value for Λ is far beyond the Planck mass $O(10^{19})$ GeV for which gravity cannot be neglected. Certainly new physics comes into play at the Planck scale, so effectively the regulator scale for $m_{\rm H} = 100$ GeV may be considered to be irrelevantly high. On the other hand, when $m_{\rm H}$ increases, Λ decreases. When $\lambda_{\rm R}$ becomes too large eq. (3.189) can no longer be trusted, but we still have non-perturbative results for $\lambda_{\rm R}$ and the corresponding $\Lambda/m_{\rm H}$ anyhow. For example, for $m_{\rm H} = 615$ GeV ($m_{\rm H}/v_{\rm R} = 2.5$) figure

3.17 shows that $1/am_{\mathrm{H}} \approx 3$; hence $\Lambda \approx 3\pi m_{\mathrm{H}} = 5800$ GeV, for the standard action. For the Symanzik-improved action this would be $\Lambda \approx 8300$ GeV.

So we can compute a cutoff scale Λ from knowledge of the Higgs mass, but this Λ is clearly regularization dependent (the dependence of C in (3.189) on λ_0 also indicates a regularization dependence, cf. c in eq. (3.146)). For values of m_{H} deep in the scaling regime Λ is very sensitive to changes in m_{H}, but at the edge of the scaling region, e.g. for $\Lambda/m_{\mathrm{H}} \approx 6$, this dependence is greatly reduced.

This supports the idea of establishing an upper bound on the Higgs mass: given a criterion for allowed scaling violations, there is an upper bound on m_{H} [31]. For example, requiring $\Lambda/m_{\mathrm{H}} > 2\pi$ ($am_{\mathrm{H}} < \frac{1}{2}$), we get an upper bound on m_{H} from results like figure 3.17. This should then be maximized over all possible regularizations. Figure 3.17 shows that the standard and Symanzik-improved actions give the bounds $m_{\mathrm{H}}/v_{\mathrm{R}} \lesssim 2.7$ and 3, respectively. A way to search through regularization space systematically has been advocated especially by Neuberger [32]. To order $1/\Lambda^2$ all possible regularizations (including ones formulated in the continuum) can be represented by a three-parameter action on the F_4 lattice, which has more rotational symmetry than does the hypercubic lattice. It is believed that the results of this program will not lead to drastic changes in the above result $m_{\mathrm{H}}/v_{\mathrm{R}} \lesssim 3$.

The Pauli–Villars regularization in the continuum appears to give much larger Λ's than the lattice [33]. The problem with relating various regularization schemes lies in the fact that it is not immediately clear what the physical implications of a requirement like $\Lambda/m_{\mathrm{H}} > 2\pi$ are. One may correlate Λ to regularization artifacts (mimicking 'new physics') in physical quantities, such as the scattering amplitude for the Goldstone bosons. Requiring, in a given regularization, that such an amplitude differs by less than 5%, say, from the value obtained in renormalized perturbation theory, would determine Λ and the corresponding upper bound on m_{H} in that regularization. The significance of such criteria is unclear, however.

At this point it is useful to recall one example in which nature (QCD) introduces 'new physics'. The $O(4)$ model may also be interpreted as giving an effective description of the three pions, which are Goldstone bosons with masses around 140 MeV due to explicit symmetry breaking. The expectation value v_{R} is equal to the pion decay constant, $v_{\mathrm{R}} = f_\pi = 93$ MeV. The analog of the Higgs particle is the very broad σ resonance around 900 MeV. The low-energy pion physics is approximately described by the $O(4)$ model. However, since $m_\sigma/v_R \approx 10$ is far above the upper bounds found above, the cutoff needed in this application of the $O(4)$ model is very low, probably even below m_σ, and the model is not expected to describe physics at the σ scale. Indeed, there is 'new physics' in the form of the well-known ρ resonance with a mass of 770 MeV and width of about 150 MeV.

Let us now discuss the assumptions of neglecting the effect of the gauge and Yukawa couplings. The gauge couplings $g_{2,3}$ are asymptotically free and their effective size is even smaller on the scale of the cutoff. So it seems reasonable that their inclusion will not cause large deviations from the above results. The $U(1)$ coupling g_1 is not asymptotically free and its effective strength grows with the momentum scale. However, its size on the Planck scale is still small. If we accept not putting the cutoff beyond the Planck scale anyway, then also the gauge coupling g_1 may be expected to have little influence. The same can be said about the Yukawa couplings, which are also not asymptotically free (possibly with the exception of the top-quark coupling).

These expectations have been studied in some detail. An important result based on $O(4)$ Ward identities is that relations like $m_W^2 = g_2^2 v_R^2/4$ are still valid to first order in g_2^2 on treating the Higgs self-coupling non-perturbatively [31, 34]. This may be seen as justifying a definition of the g_R such that (3.186) is exact.

Of course, it is desirable to verify the above expectations non-perturbatively. A lattice formulation of the Standard Model is difficult because of problems with fermions on a lattice (cf. section 8.4). However, lattice formulations of gauge-Higgs systems and to a certain extent Yukawa models are possible and have been much studied over the years. The lattice formulation of gauge-Higgs systems has interesting aspects having to do with the gauge-invariant formulation of the Higgs phenomenon, presentation and discussion of which here would lead too far [35].

It turns out that the Yukawa couplings are also 'trivial' and that the maximum renormalized coupling is also relatively weak, see for example [36]. Numerical simulations have set upper bounds on the masses of possible hitherto undiscovered generations of heavy fermions (including heavy neutrinos), as well as the influence of such generations on the Higgs-mass bound.

Finally, the assumption made above, namely that $m_H \neq 0$, is justified by theoretical arguments for a *lower bound* on m_H, which are based on the effect that the fermions and gauge bosons induce on the Higgs self-couplings (for reviews, see [37, 38]).

3.13 Problems

(i) *Six-point vertex*

Determine the Feynman diagrams for the six-point vertex function in the φ^4 theory in the one-loop approximation. For one of these diagrams, write down the corresponding mathematical expression in lattice units ($a = 1$) and in physical units ($a \neq 1$). Show that it converges in the limit $a \to 0$, to the expression one would write down directly in the continuum.

(ii) *Renormalized coupling for mass zero*

In the massless $O(n)$ model λ_{R} is ill defined. In this case $\bar{\lambda}(\mu)$ is still a good renormalized coupling. Give the renormalized four-point vertex function $\Gamma^{\mathrm{R}}_{\alpha_1\cdots\alpha_4}(p_1 \cdots p_4)$ in terms of $\bar{\lambda}(\mu)$.

(iii) *Critical κ and m_0 at weak coupling*

What are the critical values of the bare mass $m_{0\mathrm{c}}^2$ (in lattice units) and the hopping parameter κ_{c} to first order in λ_0 in the weak-coupling expansion?

(iv) *Minimal subtraction*

To obtain renormalized vertex functions in the weak-coupling expansion, wavefunction, mass, and coupling-constant renormalizations are needed. Here we concentrate on the latter. We substitute the bare λ_0 for a series in terms of a renormalized λ (not to be confused with the λ in the lattice parameterization (3.15)),

$$\begin{aligned} \lambda_0 &= \lambda Z_\lambda(\lambda, \ln a\mu), \\ Z_\lambda(\lambda, \ln a\mu) &= 1 + \sum_{n=1}^{\infty} \sum_{k=0}^{n} Z_{nk} \lambda^n (\ln a\mu)^k \\ &= \sum_{k=0}^{\infty} Z_k(\lambda)(\ln a\mu)^k. \end{aligned} \tag{3.190}$$

Terms vanishing as $a \to 0$ have been neglected, order by order in perturbation theory. From the point of view of obtaining finite renormalized vertex functions we can be quite liberal and allow any choice of the coefficients Z_{nk} leading to a series in λ for physical quantities for which the a dependence cancels out.

The renormalized λ depends on a physical scale μ but not on a, it is a 'running coupling', whereas λ_0 is supposed to depend on a but not on μ. Introducing a reference mass μ_1, we write

$$\lambda_0(t) = \lambda(s) Z_\lambda(\lambda(s), s - t), \quad t = -\ln(a\mu_1), \quad s = \ln(\mu/\mu_1). \tag{3.191}$$

https://doi.org/10.1017/9781009402705.004 Published online by Cambridge University Press

From $0 = d\lambda_0/ds$ we find

$$\left(\frac{\partial}{\partial s} + \beta\,\frac{\partial}{\partial\lambda}\right)\lambda Z_\lambda(\lambda, s-t) = 0, \tag{3.192}$$

where

$$\beta = \frac{\partial\lambda}{\partial s}. \tag{3.193}$$

Using the above expansion for Z_λ in terms of powers $(\ln a\mu)^k = (t-s)^k$, show that

$$(k+1)Z_k(\lambda) + \beta\,\frac{\partial}{\partial\lambda}(\lambda Z_k(\lambda)) = 0, \quad k = 0, 1, 2, \ldots, \tag{3.194}$$

and hence that the β function is given by

$$\beta(\lambda) = -\frac{Z_1(\lambda)}{\partial(\lambda Z_0(\lambda))/\partial\lambda}. \tag{3.195}$$

In a minimal subtraction scheme one does not 'subtract' more than is necessary to cancel out the $\ln(a\mu)$'s, and one chooses $Z_0(\lambda) \equiv 1$. Notice that there is a whole class of minimal subtraction schemes: we may replace $\ln(a\mu)$ by $\ln(a\mu) + c$, with c some numerical constant, since such a c is equivalent to a redefinition of μ. It follows that the beta function in a minimal subtraction scheme can be read off from the coefficients of the terms involving only a single power of $\ln a\mu$:

$$\beta(\lambda) = -Z_1(\lambda). \tag{3.196}$$

Show that in minimal subtraction the beta function $\beta_0(\lambda_0)$ for λ_0 is identical to $\beta(\lambda_0)$.

Assuming that the beta function is given, solve eq. (3.192) with the boundary condition $Z_\lambda(\lambda, 0) = Z_0(\lambda) = 1$.

(v) *Mass for small κ*

The hopping result (3.128) shows that the mass parameter $m_{\rm R}$ is infinite for $\kappa = 0$. For small κ we see from (3.122) that $G_{xy} \propto (2g\kappa)^{L_{xy}} = \exp(-m_{xy}|x-y|)$, where L_{xy} is the minimal number of steps between x and y. We can identify a mass $m_{xy} = -\ln(2g\kappa)\,(L_{xy}/|x-y|)$. For small κ, compare m_{xy} for x, y along a lattice direction and along a lattice diagonal with the results of problem (i) in chapter 2. Compare also with equations (2.117), (2.120) and (2.122), for the case that x and y are along a timelike direction in the lattice.

(vi) *An example of a divergent expansion*
Instructive examples of convergent and divergent expansions, in κ and λ, are given by

$$z(\kappa, \lambda) = \int_{-\infty}^{\infty} d\phi \exp(-\kappa\phi^2 - \lambda\phi^4) \tag{3.197}$$

$$= \frac{\lambda^{-1/4}}{2} \sum_{k=0}^{\infty} \frac{\Gamma(k/2 + 1/4)}{k!} (-\kappa\lambda^{-1/2})^k \tag{3.198}$$

$$= \kappa^{-1/2} \sum_{k=0}^{\infty} \frac{\Gamma(2k + 1/2)}{k!} (-\lambda\kappa^{-2})^k. \tag{3.199}$$

Verify.

(vii) *A dimension-six four-point vertex*
Show that the dimension-six term $-\sum_x a^2\lambda_0 z \partial_\mu \varphi_x^2 \partial_\mu \varphi_x^2$ in the general action (3.173) corresponds to the vertex function

$$^0\Gamma(p_1 \cdots p_4) = -8a^2\lambda_0 z(-i)^2 K_\mu^*(p_1 + p_2) K_\mu^*(p_3 + p_4)$$
$$+ \text{two permutations}, \tag{3.200}$$

$$K_\mu(p) = \frac{1}{ia}(e^{iap_\mu} - 1). \tag{3.201}$$

In the classical continuum limit this vertex vanishes but in one-loop order it contributes to the two-point function $\Gamma(p)$ (cf. figure 3.5). Show that this contribution is given by

$$+4\lambda_0 z \left[2a^{-2} + p^2\left(C_0 - \tfrac{1}{8}\right) + O(a^2)\right], \tag{3.202}$$

where C_0 is given in (3.67) and we used $(2\pi)^{-4} \int_{-\pi}^{\pi} d^4 l\, \hat{l}_\mu^2 / \hat{l}^2 = \frac{1}{4}$, independent of $\mu = 1, \ldots, 4$.

(viii) *Langevin equation and Fokker–Planck Hamiltonian*
Consider a probability distribution $P(\phi)$ for the field ϕ_x. One Langevin time step changes ϕ into ϕ' according to

$$\phi_x' = \phi_x + \sqrt{2\delta}\, \eta_x + \delta \frac{\partial S(\phi)}{\partial \phi_x}. \tag{3.203}$$

This corresponds to $P(\phi) \to P'(\phi)$. The new $P'(\phi)$ may be determined as follows. Let $O(\phi)$ be an arbitrary observable, with average value $\int D\phi\, P(\phi) O(\phi)$. After a Langevin time step the new average value is $\int D\phi\, P(\phi) \langle O(\phi'(\phi))\rangle_\eta$, where $\langle \cdots \rangle_\eta$ denotes the average over the Gaussian random numbers η_x. By definition this new average value is equal to $\int D\phi\, P'(\phi) O(\phi)$, i.e.

$$\int D\phi\, P'(\phi) O(\phi) = \int D\phi\, P(\phi) \langle O(\phi'(\phi))\rangle_\eta. \tag{3.204}$$

By expansion in $\sqrt{\delta}$, show that

$$\langle O(\phi')\rangle_\eta = O(\phi) + \delta \sum_x \left[\frac{\partial O(\phi)}{\partial \phi_x}\,\frac{\partial S(\phi)}{\partial \phi_x} + \frac{\partial^2 O(\phi)}{\partial \phi_x\,\partial \phi_x}\right] + O(\delta^2), \tag{3.205}$$

and consequently that

$$\frac{P' - P}{\delta} = \sum_x \frac{\partial}{\partial \phi_x}\left[\frac{\partial}{\partial \phi_x} - \frac{\partial S}{\partial \phi_x}\right] P \tag{3.206}$$

$$\equiv -H_{\mathrm{FP}}\,P. \tag{3.207}$$

The partial differential operator in ϕ-space, H_{FP}, is called the Fokker–Planck Hamiltonian. Using

$$\frac{\partial}{\partial \phi_x}\,e^{S/2} = e^{S/2}\left(\frac{\partial}{\partial \phi_x} + \frac{1}{2}\,\frac{\partial S}{\partial \phi_x}\right), \tag{3.208}$$

show that $\tilde{P}$ defined by $P = e^{S/2}\tilde{P}$ satisfies

$$\frac{\tilde{P}' - \tilde{P}}{\delta} = -\tilde{H}\tilde{P} + O(\delta), \tag{3.209}$$

$$\tilde{H} = \sum_x \left(-\frac{\partial}{\partial \phi_x} - \frac{1}{2}\,\frac{\partial S}{\partial \phi_x}\right)\left(\frac{\partial}{\partial \phi_x} - \frac{1}{2}\,\frac{\partial S}{\partial \phi_x}\right).$$

Show that $\tilde{H}$ is a Hermitian positive semidefinite operator, which has one eigenvalue equal to zero with eigenvector $\exp(S/2)$. Give arguments showing that, as $\delta \to 0$ and the number n of iterations goes to infinity, with $t = n\delta \to \infty$, P will tend to the desired distribution $\exp S$.

https://doi.org/10.1017/9781009402705.004 Published online by Cambridge University Press